RÉPUBLIQUE ALGÉRIENNE DÉMOCRATIQUE ET POPULAIRE
MINISTÈRE DE L'ENSEIGNEMENT SUPÉRIEUR ET DE LA RECHERCHE SCIENTIFIQUE
UNIVERSITÉ MOHAMED BOUDIAF - M'SILA
FACULTÉ DE MATHÉMATIQUES ET DE L'INFORMATIQUE
DÉPARTEMENT DE MATHÉMATIQUES

N° d'ordre: .....

T H È S E

Présentée pour l'obtention du diplôme
de Doctorat troisième cycle
Spécialité:
Mathématiques
Option:
Mathématiques et applications
Par:
Rafaa Chouder
Thème

Auto-Similarité et Contour d'Image

"Self-Similarity and Image Contour"

Soutenue publiquement le : 11/02/ 2018, devant le jury :

Gasmi Abd Elkader	Prof.,	U. M'sila	Président
Benhamidouche Noureddine	Prof.,	U. M'sila	Rapporteur
Benterki Djamel	Prof.,	U. Sétif	Examinateur
Hachama Mohammed	M.C.A.,	U. Khemis Miliana	Examinateur
Merzougui Abd Elkarim	M.C.A.,	U. M'sila	Examinateur

Promotion 2017/2018

Acknowledgement

All praise and gratitude is due to Allah, and I want to thank all the people who played a part in this adventure. First, I am deeply grateful to my supervisor, Prof. Benhamidouche Noureddine for his guidance, encouragement and patience during the preparation of my thesis, and for introducing me to this field. Also, my thanks and appreciation goes to my thesis committee members: Prof. Gasmi Abd Elkader, Prof. Benterki Djamel, Dr. Merzougui Abd Elkarim, Dr. Hachama Mohammed, and I wish to pay my great appreciation to all respected teachers in department of mathematics in M'Sila university. Finally, I would like to thank my family and my friends for their encouragement.

Table of Contents

Introduction

Many models using nonlinear diffusion equations are proposed in image processing and contour enhancement [31, 19, 8, 28, 1]. PDE-base techniques for edge detection has been firstly introduced by Perona and Malik [25]. They proved that image intensity flux can lead to an enhancement of image edge if the flux is in opposite direction of image intensity gradient. Different approaches to edge enhancement were proposed by several authors. In particular, Malladi and Sethian [21] proposed a model based on a differential-geometric approach. The asymptotic treatment of these models, shows the enhancement of the intensity contrast by formation of regions of large intensity gradient.

In order to focus on the boundary layer where large gradients concentrate, further simplifications of this model were proposed [3], and lead to the following unidimensional PDE:

$$\frac{\partial u}{\partial t} = u_x^{-2(1+\gamma)} u_{xx}. \tag{0.0.1}$$

This equation governs the evolution of the image intensity in the boundary layer. It turns out that the standard initial value problem solved in this theory does not fit the present application since it does not produce image concentration. In the range of exponents $\gamma > -1$, equation (0.0.1) falls into the class of degenerate parabolic equations with degeneracy at $u_x = \infty$. Due to the degenerate character of the diffusivity at high gradient values, a free boundary problem can be introduced describing the image intensity evolution in the boundary layer.

To analyze the process of contour enhancement in image processing for $\gamma > 0$. Analysis of intermediate-asymptotic solutions, introduced by Barenblatt [3], for the image evolution

in the boundary layer of an image demonstrated that the edge enhancement takes place for the class of flows under consideration. The rate of enhancement depends on the parameter, i.e., on the hypotheses concerning the image intensity flow.

In this work, we first suggest to find exact solutions to a nonlinear diffusion equation that occurs in image processing by using general self-similar solutions and introducing the "Travelling profiles solutions" [5, 6], to seek exact solutions for some nonlinear partial differential equations. On the other hand, we want to generalize the results proposed in [3], and we show that such behaviors can be observed in the larger exponent range $\gamma > -1$. We note that this problem for $\gamma > \frac{-1}{2}$ has been investigated by Barenblatt and Vasquez in [4] but with complicate conjugate formulation.

This work is divided into 4 chapters. Chapter one deals with the nonlinear diffusion equation and its using in the theory of contour enhancement in image processing. Here we give some basic concepts and models of filtering based to the theory of diffusion. Asymptotic analysis of one-dimensional problem is investigated. Chapter two is devoted to the study of free boundary problem describing the image intensity evolution in the boundary layer, by introducing general self similar solutions. We recover three types of self similar solutions which describe contour enhancement in the larger exponent range of parameter γ .

In the next chapter, we, first, propose to find new exact solutions to equation (0.0.1) by introducing the "travelling profiles solutions". This form is more general than the form proposed in chapters one and two. On the other hand, we present a generalization of the results studied in previous chapters. We based in this chapter on the work published in *'International Journal of Computing Science and Mathematics'* [11].

The last chapter is devoted to the study of more general case when we introduce the fractional derivative in the theory of contour enhancement. We suggest to find new exact solutions for fractional diffusion equation.

Chapter 1

Nonlinear diffusion in contour enhancement and image processing

Many mathematicians have been attracted by image processing and computer vision in recent years. This has been triggered by mathematically well-founded methods using e.g. wavelets or nonlinear partial differential equations, the latter being either stationary (usually minimization problems) or evolution equations.

The nonlinear diffusion technique has evolved in a very fruitful way. It is closely connected to a specific kind of multi-scale analysis called scale-space (with respect to the time variable of the nonlinear PDE), and it has been used for image smoothing with simultaneous edge enhancement. Later on, close connections to regularization methods have been discovered, and related nonlinear methods have also entered computer vision fields such as motion analysis in image sequences or interactive segmentation.

In image processing, it is generally desirable to smooth the homogenous regions of the picture with tow scopes: noise elimination and image interpretation (pattern recognition). On the other side, we wish to keep the accurate location of the boundaries of these regions. Those boundaries are called "step edges". In the classical theory, these objects are defined as the curves where the gradient of the smoothed picture has a maximum. ("Edge point" is therefore related to the property that the Laplacian of the smooth signal at that point changes sign).

1.1 The Image Society

Faced with a society in evolution ever faster, our society very well be considered as an image society. This is not only due to image is power and importance as a mean of communication but also for it is so easy, compact, and very famous existing tool used by all the people and everywhere to describe, express and represent the physical world. It captures a moment, an event that it freezes and offers us to analysis, to ameliorate their quality, enhance some characteristics to efficiently combine different pieces of information. Advertising, Photography, video games, ..etc, our daily lives of images.

We could also mention many different applications where image processing is concerned. For examples, medical imaging, satellite and aerial imaging, forecasting the weather, fingerprint analysis, robotics, quality control, Multimedia data management, video processing, restoration of old movies, etc. (See Figure 1)[2].

Without necessarily knowing it, we are consumers of image processing on a daily basis.

1.1.1 Image processing

The goal of image processing and computer vision is to process images in such a way that they are easier to interpret by human beings or better to process by further algorithms. Computer Vision tries to do what a human brain does with the retinal input, it includes understanding and predicting the visual input. That could consist of segmentation, recognition, reconstruction (3D) and prediction (over video data). Classically, many Computer Vision algorithms employed image processing and machine learning or sometimes other methods (e.g Variational Methods, Combinatorial approaches,...) to do the mentioned tasks.

Image processing focuses on enhancing the quality of single images. Image processing algorithms are used for:

- extraction of important image structures such as edges and corners (since the human visual system is very sensitive to this kind of discontinuities),

Figure 1: Illustration of some applications or systems that use image analysis.

- segmentation: dividing the image into regions of constant color where one has discontinuities at the region boundaries,
- deblurring: Reconstruction of a visually better image from a blurred image (since in a blurred image edges are smeared and dislocated),
- denoising: Removing noise from a noisy image.

1.1.2 Mathematical representation of an image

In image processing, a continuous gray-scale image is considered that is a two-dimensional function:

$$\begin{aligned} u &: \mathbb{R}^2 \to [0;1] \\ &(x,y) \to u(x,y) \end{aligned}$$

The variable (x, y), for digital images, actually belongs to $\mathbb{N}^2$, it is a pixel of the image. $u(x, y)$ represents the luminous intensity, or the gray level of the image at the pixel (x, y).

Digital images are most commonly presented as a matrix of scalars for gray-scale images or vectors for color images. Digital gray scale images on the other hand are sampled and quantized. Sampling is the discretization of the image domain. Here an image consists of gray values of a rectangular point grid $\{u_{i,j} \setminus \ i = 0, ..., N-1 \text{ and } j = 0, ..., M-1\}$. A grid point (i, j) is called pixel. Here N and M is the width and height of the image in pixels, respectively. $u_{i,j}$ denotes the gray value of pixel (i, j). (See Figure 2).

For a color image, it is not enough to know its gray level for each pixel: it is necessary to know the intensity of each of the three channels of the fundamental colors, the red **R**, the green **G**, and the blue **B**. An color image can then be defined as a vector function

$$\begin{aligned} u &: \mathbb{R}^2 \to [0;1]^3 \\ &(x,y) \to u(x,y) = (R(x,y); G(x,y); B(x,y)) \end{aligned}$$

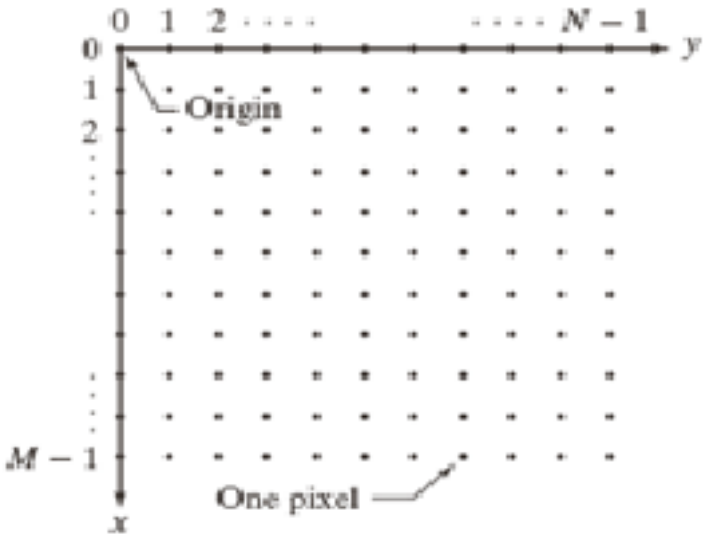

Figure 2: A matrix representation for the image

1.2 Nonlinear diffusion filtering

1.2.1 Diffusion as a physical phenomenon

Nonlinear diffusion equations, as an important class of parabolic equations, come from a variety of diffusion phenomena appeared widely in nature. They are suggested as mathematical models of physical problems in many fields such as filtration, phase transition, biochemistry and dynamics of biological groups.

Diffusion is a physical process equilibrating concentration differences in a medium while preserving the total mass of that medium. In the other words, the term diffusion is used to describe the transportation of mass, which equilibrates concentration differences without creating of destroying mass [30]. This physical observation can be translated into the following equation:

$$j = -D\nabla u, \tag{1.2.1}$$

where D is the diffusion coefficient which describes the relation between ∇u, the gradient of the concentration of mass u, and the flux density j. Says that a concentration gradient ∇u causes a flux j which aims to compensate this gradient. This equation is known as

fick's law of diffusion. The continuity equation,

$$\frac{\partial u}{\partial t} = -\operatorname{div} j, \tag{1.2.2}$$

where t is the time and div denotes the divergence operator, expresses the idea that: Diffusion does only transport mass without destroying it or creating new mass.

We know from basic calculus that the divergence of a function $u(x, y)$ is equal to the scalar product of the divergence operator ∇ and the function u:

$$\operatorname{div} u = \nabla . u = \frac{\partial u}{\partial x} + \frac{\partial u}{\partial y}. \tag{1.2.3}$$

Substitution of fick's law into the continuity equation, yields the following diffusion equation (Fick's second law of diffusion):

$$\frac{\partial u}{\partial t} = \operatorname{div}\left(D \nabla u\right), \tag{1.2.4}$$

The second law states that how the concentration u changes with time. This is the general diffusion equation for many physical transport processes.

Diffusion has deservrdly attracted much attention in the field of image processing for its ability to reduce noise and enhance edges. Equation (1.2.4) and other forms derived from it descripe a large class of image processing operations, where we may identify the concentration u with the grey value of the image at a certain location (x, y). " for gray-scale images ". If the diffusion coefficient D is constant over the whole image domain, then the diffusion does not depend of the evolving image, the process is equivalent to the linear scale space which is know as linear filtring (cf. [31]). If the diffusion coefficient D is a function depends on the evolving image, the equation (1.2.4) leads to a nonlinear diffusion filter [30].

1.2.2 Linear diffusion filtering

The first step to use PDEs for smoothing images was donne in the beginning of eighties, when the idea of scale-space filtering has introduced by Witkin [31] and further developed by Koenderink [19].

The essential idea of this approach is quite simple: embed the original image in a family of derived images $u(x, y, t)$ obtained by convolving the original image $u_0(x, y)$ with a Gaussian kernel $G_{\sqrt{2t}}(x, y)$ of variance t:

$$u(x, y, t) = \left(G_{\sqrt{2t}} * u_0\right)(x, y)\,, \tag{1.2.5}$$

where

$$G_\sigma(x, y) = \frac{1}{2\pi\delta^2} \exp\left(-\frac{(x^2 + y^2)}{2\sigma^2}\right). \tag{1.2.6}$$

This family of derived images may equivalently be viewed as the solution of the following heat equation or the linear diffusion equation

$$\begin{cases} \frac{\partial u}{\partial t} = \triangle u \\ u(x, y, 0) = u_0(x, y) \end{cases}, \tag{1.2.7}$$

for a function $u(x, y, t)$ is the smoothed image at t, and $\triangle = \frac{\partial^2}{\partial x^2} + \frac{\partial^2}{\partial y^2}$ denote Laplacian operator, with the initial condition $u(x, y, 0) = u_0(x, y)$, the original image.

Koenderink [19] motivates the diffusion equation formulation by stating two criteria:

1. **Causality**: Any feature at a coarse level of resolution is required to possess a (not necessarily unique) "cause" at a finer level of resolution although the reverse need not be true. In other words, no spurious detail should be generated when the resolution is diminished.

2. **Homogeneity and Isotropy**: The blurring is required to be space invariant.

The linear diffusion filter has its limitations: whether we smooth uniformly by a rotational symmetric Gaussian kernel, or diffuse the data equally in all directions, the process not only removes undesirable local extrema (noise) but also deforms important features of the image, blurs and dislocates edges. To overcome these drawbacks, we have to move to nonlinear filters; nonlinear diffusion offers an excellent alternative.

1.2.3 Nonlinear diffusion filtering

Overcoming the undesirable effects of linear smoothing filtering, such as blurring or dislocating the semantically meaningful edges of the image, nonlinear diffusion equations can be used because the nonlinear diffusion technique not only preserves the edge sharpness, it may also enhance it. This technique was firstly proposed by Perona and Malik [25] by stating three criteria:

1. **Causality:** no spurious detail should be generated passing from finer to coarser scales.

2. **Immediate localization:** boundaries should be sharp and coincide with the semantically meaningful boundaries at that resolution.

3. **Piecewise smoothing:** intra-region smoothing should be preferred to interregion smoothing.

To satisfy the second and third criteria, Perona and Malik proposed to change the diffusion coefficient D, (D is constant in linear diffusion); by introducing a space-time-variant diffusion coefficient. Therefore the Perona-Malik model can be written as

$$\begin{cases} \frac{\partial u}{\partial t} = \ div(g\left(|\nabla u|\right)\nabla u) \\ \quad u(x,y,0) = u_0(x,y) \end{cases}, \tag{1.2.8}$$

where div denotes the divergence operator, $u(x,y,t)$ is the smoothed image at time step t, $|\nabla u|$ is the gradient magnitude of u, and $g(x)$ is the diffusivity function. $g(x)$ should be a nonnegative, monotonically decreasing function with $g(0) = 1$, so that the diffusion is maximal within uniform regions, and approaching *zero* at infinity, so that the diffusion is stopped across edges.

In order to establish the results concerning the enhancement of edges in Perona-Malik model, we analyze the way in which the gradients in the edge region evolve with time t. In other words, we need to find the function of $\frac{\partial(u_x)}{\partial t}$.

In the case of a 1-D signal, the Perona-Malik diffusion equation can be written as

$$\begin{aligned} \frac{\partial u}{\partial t} &= \frac{\partial}{\partial x}\left(g(u_x)u_x\right) \\ &= \frac{\partial g(u_x)}{\partial x}u_x + g(u_x)u_{xx}. \end{aligned} \tag{1.2.9}$$

For ease of understanding, we define the flux function $\phi(x) = g(x).x$, where $g(x)$ is the diffusivity function. Therefore, we can write (1.2.9) as follow

$$\frac{\partial u}{\partial t} = \phi'(u_x)u_{xx}. \tag{1.2.10}$$

The change of the gradients, at any location of the edge, is given by:

$$\frac{\partial\left(u_x\right)}{\partial t} = \phi''(u_x)u_{xx}^2 + \phi'(u_x)u_{xxx}. \tag{1.2.11}$$

The sign of the right hand-side of equation (1.2.11) tells us whether a gradient u_x at location x is increasing $\left(\frac{\partial(u_x)}{\partial t} > 0\right)$ or decreasing $\left(\frac{\partial(u_x)}{\partial t} < 0\right)$, which means that the blurring/enhancing behaviour of the Perona-Malik filter depends on the sign of $\phi'(u_x)$.

On the edge, the second derivative $u_{xx} = 0$ and $u_{xxx} \leq 0$ since at this point the gradient is maximum (See Figure 3). The gradient at the edge decreases if $\phi'(u_x) > 0$, so the edge is blurred. If $\phi'(u_x) < 0$, the gradient at the edge increases with time while the neighboring gradients decrease, this process leads to sharp edges.

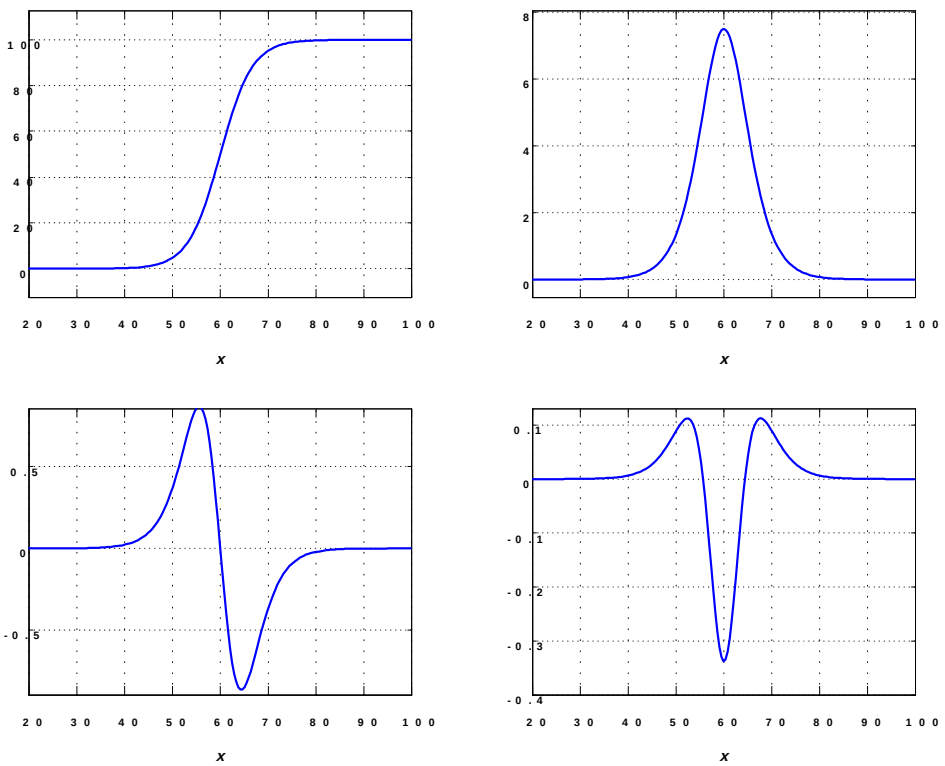

Figure 3: The edge function $u(x)$ and its first, second, and third derivatives, in the top left, top right, bottom left, and bottom right, respectively.

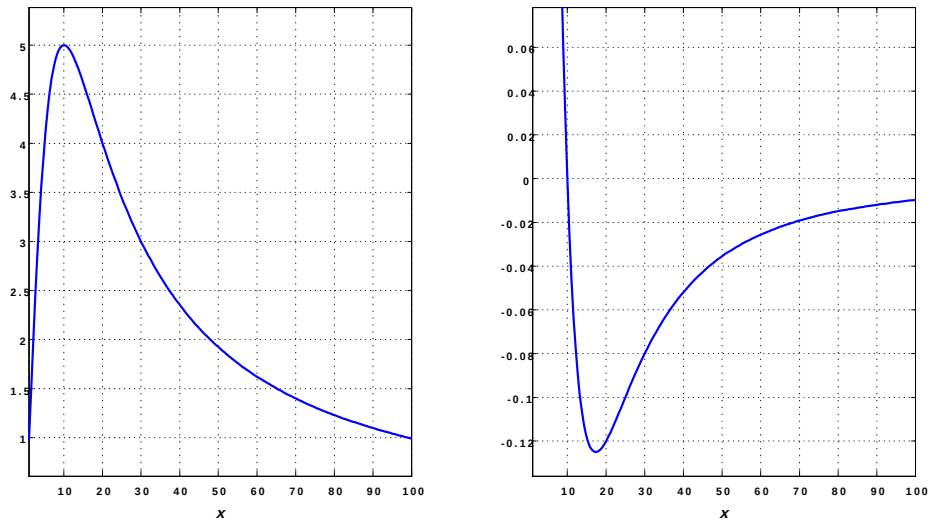

Figure 4: Flux function ϕ (left) and its derivative ϕ' (right).

Nonlinear diffusion filtering can successfully smooth noise while respecting the region boundaries and small structures within the image, as long as some of its crucial parameters are determined or estimated correctly. According to Perona and Malik the choice of functions g for which ϕ satisfies some properties leads to the desirable result of edges enhancement. The most commonly used diffusivity functions in the literature are listed in the following Table.

Function	Reference
$g(x) = 1$	Linear Diffusion
$g(x) = \frac{1}{\sqrt{1+\frac{x^2}{\delta^2}}}$	[10]
$g(x) = \frac{1}{1+\frac{x^2}{\delta^2}}$	[25]
$g(x) = exp\left(-\frac{x^2}{\delta^2}\right)$	[25]
$g(x) = \begin{cases} 1 - \exp\left[\frac{-3.15}{\left(\frac{x}{\delta^2}\right)^4}\right], & x > 0 \\ 1 & x \leq 0 \end{cases}$	[30]
$g(x) = 0.5\left[(\tanh\left[0.2(\delta - x)\right]) + 1\right]$	[13]
$g(x) = \begin{cases} \frac{1}{2}\left[1 - \left(\frac{x}{\delta}\right)^2\right]^2, & \lvert x\rvert > \delta \\ 0 & otherwise \end{cases}$	[7]
$g(x) = \begin{cases} \frac{P(T+\varepsilon)^{P-1}}{T}, & x < T \\ \frac{P(x+\varepsilon)^{P-1}}{x}, & x \geq T \end{cases}$	[32]
$g(x) = \begin{cases} \frac{P(T+\varepsilon)^{P-1}}{T} + \frac{1}{T}, & x < T \\ \frac{P(x+\varepsilon)^{P-1}}{x} + \frac{1}{x}, & x \geq T \end{cases}$	[32]

Note: δ is known as the noise threshold or the contrast parameter. T and P are parameters used to meet the requirements of the well-posedness.

1.2.4 Linear versus Nonlinear diffusion

For a useful comparison between the linear and nonlinear diffusion filtering methods and their impact on edge sharpness, we give two examples, the first for the noisy 1-D edge

profile (signal) $u(x)$ function and its filtered versions (See Figure 5(a)), the second for a gray-scale image filtred by linear and nonlinear diffusion (See Figure 5(b)).

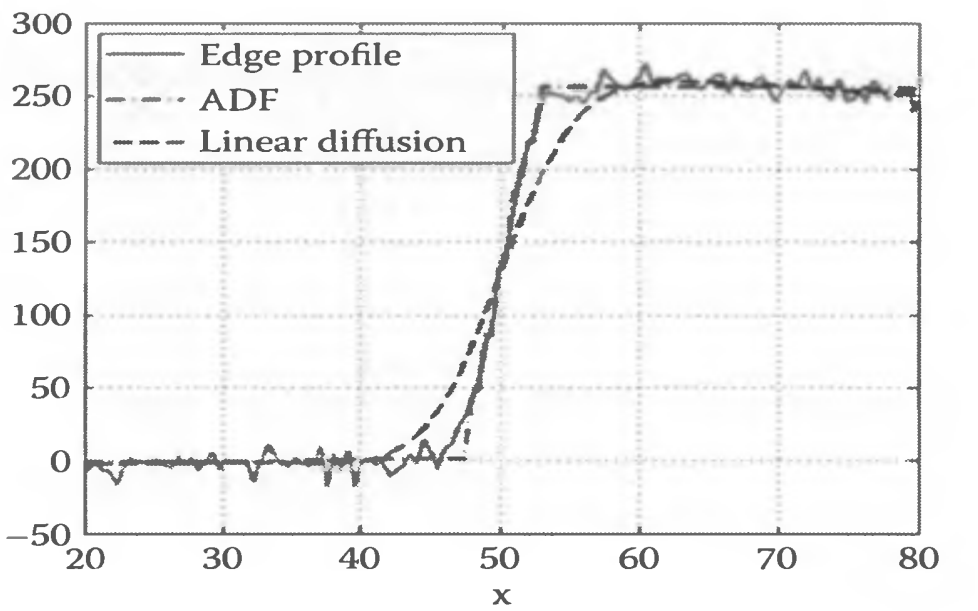

Figure 5(a): The 1-D edge profile $u(x)$ (solid) and its filtered versions. Nonlinear diffusion filtering (ADF) (dot-dash) and linear diffusion filtering (dashed).

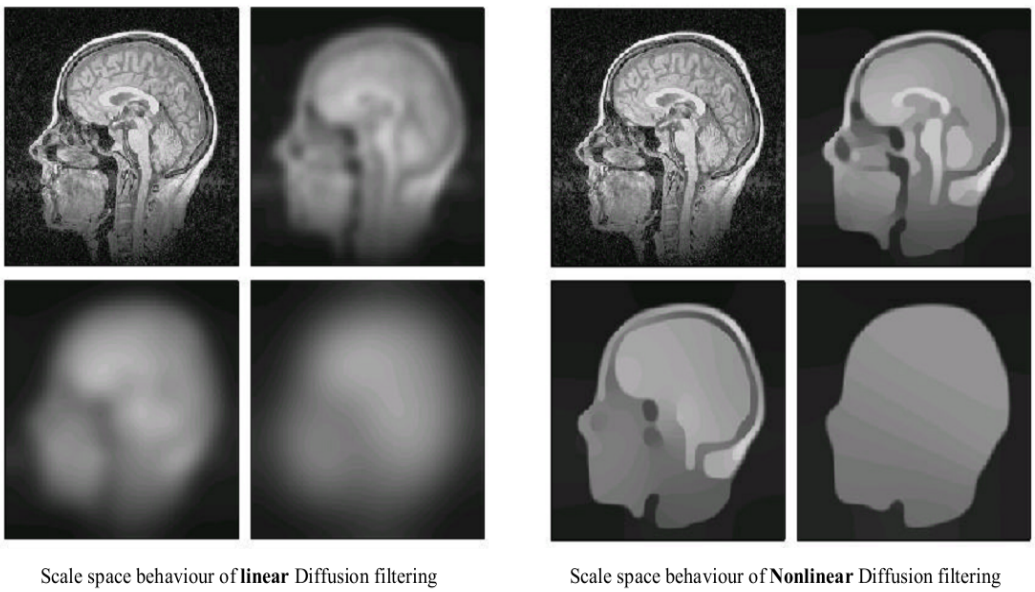

Figure 5(b): gray-scale image and its filtered versions. Linear diffusion filtering (Left) and nonlinear diffusion filtering (Right).

As seen in the figures 4 and 5, the linear diffusion filtering blurs the edge, whereas the nonlinear diffusion filtering preserves edge sharpness.

The model of Malik and Perona had several serious, practical and theoretical difficulties.

1. Assume that the signal is noisy, with the white noise for instance. Then large gradients $|\nabla u|$ are introduced by the noise. Moreover, ∇u is in theory unbounded. Thus, the conditional smoothing introduced by the model will not give good results, since all these noise edges will be kept.

2. The second difficulty arose from the equation itself. The function g needs to be considered carefully to obtain the available theory. Indeed, in order to obtain both existence and uniqueness of the solutions, g must verify that $x.g(x)$ is nondecreasing. In practice we will find out that if for some function g with $x.g(x)$ nonincreasing, very close pictures could produce divergent solutions and therefore different edges [9].

1.3 Mean curvature diffusion

An important improvement in the theory of edge enhancement is due to Malladi and Sethian [21]. They arrived (after proper scaling) to the following equations for image intensity u :

$$\frac{\partial u}{\partial t} = \left(1 + |\nabla u|^2\right)^{1/2} k, \tag{1.3.1}$$

where k denote the curvature of the surface $z = u(x, y)$ given by:

$$k = \operatorname{div}\left(\frac{\nabla u}{\sqrt{1 + |\nabla u|^2}}\right) \tag{1.3.2}$$

This equation represents movement by curvature (mean curvature flow) and can be written as:

$$
\begin{aligned}
\frac{\partial u}{\partial t} &= \sqrt{1+|\nabla u|^2}\,\mathrm{div}\left(\frac{\nabla u}{\sqrt{1+|\nabla u|^2}}\right) \qquad (1.3.3)\\
&= \sqrt{1+u_x^2+u_y^2}\,\mathrm{div}\left(\frac{u_x}{\sqrt{1+u_x^2+u_y^2}},\frac{u_y}{\sqrt{1+u_x^2+u_y^2}}\right)\\
&= \frac{1+u_x^2+u_y^2}{\sqrt{1+u_x^2+u_y^2}}\left(\frac{u_{xx}\sqrt{1+u_x^2+u_y^2}-\frac{u_xu_{xx}+u_xu_yu_{xy}}{\sqrt{1+u_x^2+u_y^2}}}{\sqrt{1+u_x^2+u_y^2}}-\frac{u_{yy}\sqrt{1+u_x^2+u_y^2}-\frac{u_yu_{yy}+u_xu_yu_{xy}}{\sqrt{1+u_x^2+u_y^2}}}{\sqrt{1+u_x^2+u_y^2}}\right)\\
&= \frac{\sqrt{1+u_x^2+u_y^2}\,(u_{xx}+u_{yy})-\frac{u_x^2u_{xx}+2u_xu_yu_{xy}+u_y^2u_{yy}}{\sqrt{1+u_x^2+u_y^2}}}{\sqrt{1+u_x^2+u_y^2}}\\
&= \frac{(1+u_y^2)u_{xx}-2u_xu_yu_{xy}+(1+u_x^2)u_{yy}}{1+u_x^2+u_y^2},
\end{aligned}
$$

As a result of a certain degeneracy of the asymptotic forms this equation, Barenblatt [3] have proposed the more general flow given by:

$$\frac{\partial u}{\partial t} = \left(1+|\nabla u|^2\right)^{(1-2\gamma)/2} k, \qquad (1.3.4)$$

where $\gamma > 0$ is a constant parameter. In the other words, it is appropriate to consider a more general class of equations:

$$\frac{\partial u}{\partial t} = \frac{(1+u_y^2)u_{xx}-2u_xu_yu_{xy}+(1+u_x^2)u_{yy}}{\left(1+u_x^2+u_y^2\right)^{1+\gamma}}. \qquad (1.3.5)$$

Along with the former case $\gamma = 0$ (mean curvature flow), the case $\gamma = 1$ has also attracted the attention of researches (Beltrami flow, cf. Sochen et al. [28]). Here, x and y are the cartesian coordinates in the image plane, t is time. Thus, according to [21], image processing is reduced to the solution of the chosen equation under an initial condition $u(x, y, 0) = u_0(x, y)$ corresponding to a grey level of the image being processed.

1.3.1 The asymptotic form of the basic equation

An analysis of images presented in [21] showed that near the edges of the images always exists a boundary layer (see Figure 7), where the normal component of the image intensity

gradient is large. This phenomenon was analyzed in [3], where a further simplification of the model, (equation (1.3.5)), was proposed in order to focus on the boundary layer where large gradients concentrate.

At the edge, using the cartesian coordinates and choosing the x-axis as the direction normal to the boundary layer, the effect of y derivatives can be neglect with respect to the x derivatives in (1.3.5). In this way, equation (1.3.5) in the boundary layer is reduced to the one-dimensional form

$$u_t(x,t) = \frac{u_{xx}}{(1+u_x^2)^{1+\gamma}}. \tag{1.3.6}$$

A configuration with large gradients makes it possible to further simplify the expression $(1+u_x^2)$ into u_x^2, so that the asymptotic form of equation (1.3.5) is obtained

$$\frac{\partial u}{\partial t} = u_x^{-2(1+\gamma)} u_{xx}. \tag{1.3.7}$$

Equation (1.3.7) governing the evolution of the image intensity in the boundary layer.

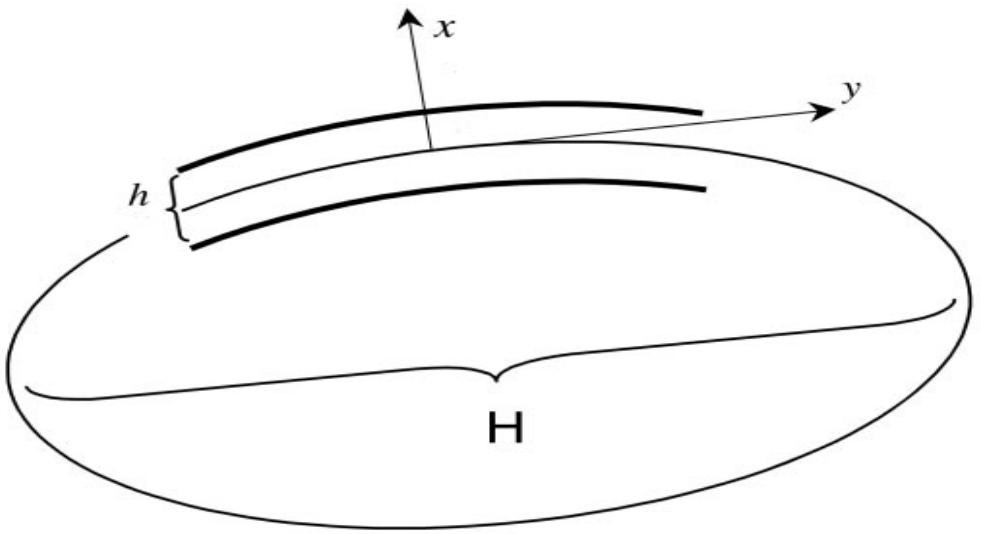

Figure 7: The boundary layer at the image edge.

To study contour enhancement in model (1.3.5), it should be resolve equation (1.3.7) for knowing important asymptotics properties of the image evolution in the boundary layer at the image edge.

1.3.2 Intermediate-Asymptotic Solutions

To study contour (edge) enhancement, it is necessary to know how the gradient and its support evolve with time. For that, an intermediate-asymptotic solution based on the dimensional analysis was proposed by Barenblatt [3], to find an exact solution of Eq.(1.3.7) under the following initial and boundary conditions:

$$u(x,-t_0)=\begin{cases} c_0, & -\infty < x \le -a \\ u_0(x), & -a \le x \le b \\ c_1, & b \le x < \infty \end{cases} \tag{1.3.8}$$

$$u(-\infty,t)=c_0,\ u(\infty,t)=c_1.$$

With, $c_0 > c_1 \ge 0$ and $a, b > 0$ are constant parameters of the problem, and the function $u_0(x)$ is assumed to be smooth at $-a \le x \le b$, so that $u_0(-a)=c_0$, $u_0(b)=c_1$. Also, it is assumed that $u_0'(-a)=c_0$, $u_0'(b)=c_1$ are negatives. c_1 can be assumed to be equal to zero.

Dimensional analysis shows that the intermediate-asymptotic solution can be represented in the form:

$$u(x,t)=c_0 f(\xi),\ \text{with}\ \ \xi=\frac{(x-x_0)\,(t+t_0)^{1/2\gamma}}{c_0^{(1+\gamma)/\gamma}}, \text{and } \gamma>0. \tag{1.3.9}$$

Substitution of this form of solutions into (1.3.7) leads to the following equation for the function $f(\xi)$

$$\frac{1}{2\gamma}\xi\frac{df}{d\xi}=\frac{d^2f}{d\xi^2}\left(\frac{df}{d\xi}\right)^{-2(1+\gamma)}.$$

Easy integration gives

$$\frac{df}{d\xi}=-\frac{1}{C^{1/2}\left[1-(\xi^2/C^2)\right]^{1/2(1+\gamma)}}.$$

Here, C is an integration constant. Integration once more and using the boundary conditions $f(-C)=1$, $f(C)=0$ we obtain

$$f(\xi)=1-\left(\frac{2\gamma}{1+\gamma}\right)^{\frac{1}{2(1+\gamma)}} C^{\frac{\gamma}{1+\gamma}} \int_{-1}^{\xi/C} \frac{d\eta}{(1-\eta^2)^{\frac{1}{2(1+\gamma)}}},$$

for $-C \leq \xi \leq C$. The relation for C can be written as follow:

$$C = \left[2 \left(\frac{2\gamma}{1+\gamma} \right)^{\frac{1}{2(1+\gamma)}} \int_0^1 \frac{d\eta}{(1-\eta^2)^{\frac{1}{2(1+\gamma)}}} \right]^{-\frac{1+\gamma}{\gamma}}.$$

Returning to the variables x and t, we obtain the intermediate-asymptotic solution for arbitrary positive γ

$$u(x,t) = c_0 \left[1 - \left(\frac{2\gamma}{1+\gamma} \right)^{\frac{1}{2(1+\gamma)}} C^{\frac{\gamma}{1+\gamma}} \int_{-1}^{\frac{(x-x_0)(t+t_0)^{1/2\gamma}}{C c_0^{(1+\gamma)/\gamma}}} \frac{d\eta}{(1-\eta^2)^{\frac{1}{2(1+\gamma)}}} \right], \tag{1.3.10}$$

for

$$l(t) = x_0 - \frac{(t+t_0)^{-\frac{1}{2\gamma}}}{c_0^{\frac{1+\gamma}{\gamma}} C} \leq x \leq x_0 + \frac{(t+t_0)^{-\frac{1}{2\gamma}}}{c_0^{\frac{1+\gamma}{\gamma}} C} = r(t).$$

Relation (1.3.10) give us important asymptotic properties of the image evolution in the boundary layer at the image edge. First of all, the width of the transition region

$$r(t) - l(t) = 2C \frac{c_0^{\frac{1+\gamma}{\gamma}}}{(t+t_0)^{\frac{1}{2\gamma}}},$$

decreases with time; the step forms from an initially noisy image (Relation (1.3.8)) and the edge enhancement takes place. Furthermore, the value of $u(x_0,t)$ remains constant (the position x_0 cannot be obtained in the presented construction and requires a matching with pre-self-similar solution, e.g., by a numerical computation). Finally, the minimum of $|u_x|$:

$$|u_x| = \frac{(t+t_0)^{\frac{1}{2\gamma}}}{c_0^{\frac{1+\gamma}{\gamma}} C}; \quad \text{at } x = x_0$$

is growing with time, therefore the validity of the asymptotic Eq.(1.3.7) improves with time (see Figure 8) ([3]).

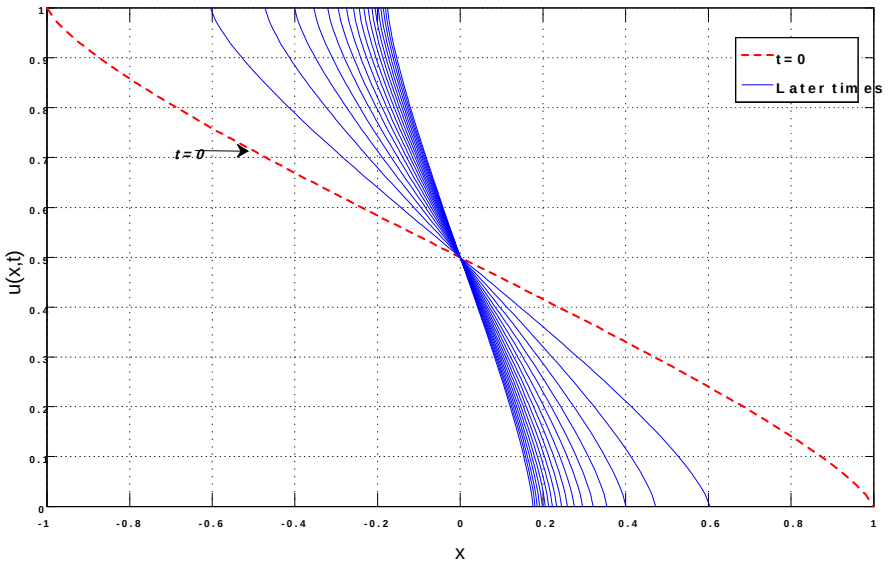

Figure 8: The evolution of the image intensity distribution $u(x,t)$ for $\gamma = 1$ "the Beltrami flow"

In the next chapter we will suggest to generalize the results obtained in [3] for larger exponent range $\gamma > \frac{-1}{2}$. We note that this case was treated in [4], with complicate conjugate formulation, they have not found the exact solutions of equation (1.3.7). For that we propose to introduce the general self similar solutions to find exact solutions for equation (1.3.7).

In our work, We have chosen the increasing profiles to avoid chasing around many minus signs.

Chapter 2

Self similar solutions and contour enhancement

In this chapter we suggest to generalize the results obtained in [3] by introducing general self similar solutions, and we show that such behaviors can be observed in the larger exponent range $\gamma > \frac{-1}{2}$. It turns out that the standard initial value problem solved in this theory does not fit the present application since it does not produce image concentration. Due to the degenerate character of the diffusivity at high gradient values, a free boundary problem can be introduced describing the image intensity evolution in the boundary layer.

2.1 Self similar solutions to nonlinear partial differential equations

Self similarity results when the symmetry of a physical problem leads to a reduction in the number of the independent variables. In this way, a considerable simplification is achieved, that frequently allows the analytical treatment of the problem. Very elegant solutions are thus derived. Usually the self similar behavior appears in the intermediate asymptotics of phenomena, when certain details of the initial or boundary conditions are

no longer relevant, so that the corresponding parameters can be ignored. The peculiarities of the passage to the limit that leads to the intermediate asymptotics of a given problem allows to classify the similarity solutions as self similarities of the first and second kind. Self similarity of the first kind can be established by dimensional analysis (eventually supplemented by other symmetry considerations). The self similarities of the second kind cannot be derived in this way: it is necessary to follow the evolution of the solution either experimentally or numerically until it passes into its self similar asymptotics, or they can be obtained by direct construction. In the second case this process leads to a nonlinear eigenvalue problem.

There is a method based on the self similar solutions which enables us to find exact solutions of PDE:

$$\frac{\partial u}{\partial t} = A_x u, \tag{2.1.1}$$

where $A_x u$ is a linear or nonlinear differential operator.

This method is largely used. Its principle is to seek a solution of (2.1.1) in the form:

$$u(x,t) = t^{\mu} f(\xi), \qquad \xi = xt^{-\nu},$$

for $x \in \mathbb{R}$, $t > 0$, where μ and ν are constants. The function f is a solution of the ODE:

$$A_\xi f - \mu f + \nu \xi f_\xi = 0.$$

There exists another form of self similar solution written under the form:

$$u(x,t) = (T-t)^{\mu} f(\xi), \qquad \xi = x\,(T-t)^{-\nu},$$

for $x \in \mathbb{R}$, $0 < t < T$, where μ and ν are constants.

The general form of self similar solutions written as follows:

$$u\,(x,t) = c\,(t)\,f\,(\xi)\,, \qquad \xi = \frac{x}{a\,(t)}, \tag{2.1.2}$$

where $c\,(t)$ and $a\,(t)$ are functions of t, chosen for reason of convenience in the specific problem.

2.2 Basic free boundary problem to contour enhancement

We introduce the following free boundary problem [4]:

Given an increasing function $u_0(x)$ defined in an interval $I = (b_1, b_2)$ with end values $u_0(b_1) = 0,\ u_0(b_2) = 1$, to find a continuous function $u(x,t)$ and continuous curves $x = l(t)$ and $x = r(t)$ such that

1. $l(0) = b_1$, $r(0) = b_2$, and $l(t) < r(t)$ for some time interval $t \in (0, T)$.

2. u solves the following problem in $\Omega = \{(x,t) : 0 < t < T,\ l(t) < x < r(t)\}$:

$$\begin{cases} \frac{\partial u}{\partial t} = u_x^{-2(1+\gamma)} u_{xx}, & \text{in } \Omega \text{ with } \gamma > \frac{-1}{2} \\ u(x,0) = u_0(x), & \text{for } \ b_1 \le x \le b_2 \\ u(l(t),t) = 0, u_x(l(t),t) = +\infty & \text{for } 0 < t < T \\ u(r(t),t) = 1, u_x(r(t),t) = +\infty & \text{for } 0 < t < T \end{cases} \tag{2.2.1}$$

This is a free boundary problem because the unknowns are the function $u(x;t)$ and the moving boundaries, $l(t)$ and $r(t)$, which must be determined from the problem thanks to the extra boundary conditions. For this reason the interfaces $x = l(t)$ and $x = r(t)$ are also called "free-boundaries".

The mathematical theory for the free-boundary problem (2.2.1) was treated in [4], with complicate conjugate formulation, where u_0 is monotone on the segment line $[b_1, b_2]$ with $u_0(b_1) = 0,\ u_0(b_2) = 1$. The problem (2.2.1) with monotone u_0 has an unique classical solution $(u; l; r)$ with $u(x,t)$ monotone [4]. The solution $u(x,t)$ sharpens as t grows; actually the two free boundaries $x = l(t)$ and $x = r(t)$ shrink. If the two moving boundaries meet, a vertical front is formed, representing completed enhancement (see Figure 9).

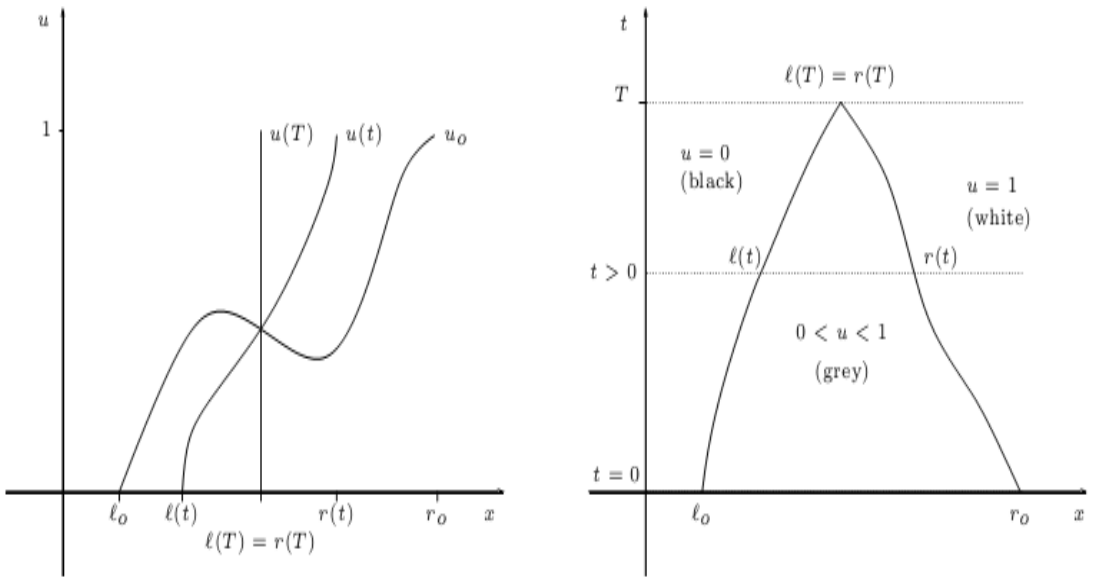

Figure 9: At the left side, the front of the solution to the free boundary problem, respectively at time 0, after some time t, and when complete enhancement occurs. At the right side, the respective sections of the grey region, i.e. the transition domain.

2.3 Contour enhancement via nonlinear degenerate parabolic equation with general self similar solutions

We try now to solve problem (2.2.1) by introducing the general form of solution (2.1.2). Taking account of this form, we obtain the following boundary conditions:

$$\begin{cases} u(l(t),t) = f(\frac{l(t)}{a(t)}) = 0,\ u_x(l(t),t) = \frac{1}{a(t)} f'(\frac{l(t)}{a(t)}) = +\infty & \text{for } 0 < t < T, \\ u(r(t),t) = f(\frac{r(t)}{a(t)}) = 1,\ u_x(r(t),t) = \frac{1}{a(t)} f'(\frac{r(t)}{a(t)}) = +\infty & \text{for } 0 < t < T. \end{cases} . \tag{2.3.1}$$

Substituting (2.1.2) into problem (2.2.1), we obtain, the equation

$$-\frac{\dot{a}}{a}\xi\frac{df}{d\xi} = \frac{1}{a^{-2\gamma}}\left(\frac{df}{d\xi}\right)^{-2(1+\gamma)}\frac{d^2f}{d\xi^2}, \quad \text{for } \gamma > -\frac{1}{2}. \tag{2.3.2}$$

A separation of variables argument implies that the following conditions must hold :

$$\frac{\dot{a}}{a} = -\beta \frac{1}{a^{-2\gamma}}, \tag{2.3.3}$$

where β is arbitrary positive constant.

The equation for the profile f, becomes:

$$\beta\xi \frac{df}{d\xi} = \left(\frac{df}{d\xi}\right)^{-2(1+\gamma)} \frac{d^2 f}{d\xi^2}. \tag{2.3.4}$$

which can be written after integration as

$$\frac{-1}{2(1+\gamma)} \left(\frac{df}{d\xi}\right)^{-2(1+\gamma)} = \beta \frac{\xi^2}{2} + k, \quad \text{with} \quad k \text{ constant.} \tag{2.3.5}$$

Finally we have

$$\frac{df}{d\xi} = \left[\frac{-1}{(1+\gamma)}\right]^{\frac{1}{2(1+\gamma)}} \left[\beta\xi^2 + K\right]^{\frac{-1}{2(1+\gamma)}}, \text{ with } K \text{ constant.} \tag{2.3.6}$$

This relation impose for $\gamma > \frac{-1}{2}$. According to different value of parameter γ, we discuss in next sections the resolution of equation (2.3.6).

The resolution of (2.3.3) gives,

$$a(t) = (2\gamma\beta t + A_0)^{\frac{-1}{2\gamma}}, \qquad \text{for } 0 < t < \infty \quad \text{if } \gamma > 0, \tag{2.3.7}$$

and

$$a(t) = (2\gamma\beta t + A_0)^{\frac{-1}{2\gamma}}, \qquad \text{for } 0 < t < T \quad \text{if } \gamma < 0, \tag{2.3.8}$$

where $A_0 > 0$, is a constant. and T is obtained as

$$T = -\frac{A_0}{2\gamma\beta}. \tag{2.3.9}$$

In the particular case $\gamma = 0$, we have:

$$a(t) = A_0 e^{-\beta t}, \qquad \text{for} \quad 0 < t < \infty. \tag{2.3.10}$$

The value of the parameter γ is important. So, we recover the self similar solutions of Type I, for $\gamma > 0$ (2.1.2) - (2.3.7) and of Type II, for $\gamma < 0$, (2.1.2) - (2.3.8), in the case $\gamma = 0$, we recover the self similar solutions of Type III (2.1.2)-(2.3.10).

We discuss below the phenomenon of contour enhancement for different value of parameter γ.

2.3.1 Self similar solution of type I

If $\gamma > 0$, we recover the self similar solution of Type I (2.3.7), that exists for all time $t > 0$.

We show below that in case $\gamma > 0$, the self similar solutions of type I, contribute to contour enhancement. We recall firstly that the parameter $a(t)$ is given by (2.3.7).

For the profile f, the equation (2.3.6) can be written as

$$\frac{df}{d\xi} = \left[\frac{1}{1+\gamma}\right]^{\frac{1}{2(1+\gamma)}} C^{\frac{-1}{1+\gamma}} \left[1 - \left(\frac{\sqrt{\beta}\xi}{C}\right)^2\right]^{\frac{-1}{2(1+\gamma)}}, \text{ with } \gamma > 0, \tag{2.3.11}$$

for

$$-\frac{C}{\sqrt{\beta}} \leq \xi \leq \frac{C}{\sqrt{\beta}}.$$

Here, C is an integration constant. For $\xi = \frac{x}{a(t)}$, we have

$$-\frac{C}{\sqrt{\beta}}a(t) \leq x \leq \frac{C}{\sqrt{\beta}}a(t). \tag{2.3.12}$$

The problem (2.3.11)-(2.3.12) suggests a free-boundary problem for determination of the image intensity evolution in the boundary layer $l(t)$ and $r(t)$ such that $l(t) \leq x \leq r(t)$, with $l(t) = -\frac{C}{\sqrt{\beta}}a(t)$ and $r(t) = \frac{C}{\sqrt{\beta}}a(t)$.

Further integration of (2.3.11) and using the boundary conditions (2.3.1), implies $f\left(-\frac{C}{\sqrt{\beta}}\right) = 0$, $f\left(\frac{C}{\sqrt{\beta}}\right) = 1$, then we obtain

$$f(\xi) = \frac{1}{\sqrt{\beta}}\left[\frac{1}{1+\gamma}\right]^{\frac{1}{2(1+\gamma)}} C^{\frac{\gamma}{1+\gamma}} \int_{-1}^{\frac{\sqrt{\beta}}{C}\xi} \frac{d\eta}{[1-\eta^2]^{\frac{1}{2(1+\gamma)}}}; \tag{2.3.13}$$

and

$$C = \left[\frac{2}{\sqrt{\beta}}\left[\frac{1}{1+\gamma}\right]^{\frac{1}{2(1+\gamma)}} \int_0^1 \frac{d\eta}{[1-\eta^2]^{\frac{1}{2(1+\gamma)}}}\right]^{-\frac{\gamma+1}{\gamma}}. \tag{2.3.14}$$

Thus, the self similar solutions of the Type I (2.1.2)-(2.3.7), assumes the form

$$u\left(x,t\right)=\frac{1}{\sqrt{\beta}}\left[\frac{1}{1+\gamma}\right]^{\frac{1}{2(1+\gamma)}}C^{\frac{\gamma}{1+\gamma}}\int_{-1}^{\frac{\sqrt{\beta}}{C}\frac{x}{a(t)}}\frac{d\eta}{\left[1-\eta^{2}\right]^{\frac{1}{2(1+\gamma)}}}. \tag{2.3.15}$$

At free boundaries $l(t)=-\frac{C}{\sqrt{\beta}}a(t)$ and $r(t)=\frac{C}{\sqrt{\beta}}a(t)$, the image intensity $u(x,t)$ is continuous. The gradients are given by

$$u_x(x,t)=\frac{1}{a(t)}\frac{df}{d\xi}\quad,$$

which can be written as

$$u_x(x,t)=\frac{1}{a(t)}\left[\frac{1}{1+\gamma}\right]^{\frac{1}{2(1+\gamma)}}C^{\frac{-1}{1+\gamma}}\left[1-\left(\sqrt{\beta}\frac{x}{Ca(t)}\right)^{2}\right]^{\frac{-1}{2(1+\gamma)}}. \tag{2.3.16}$$

We can see that, if $t\to\infty$, *then* $u_x(x,t)\to\infty$, (because $a(t)\to 0$). Therefore the validity of the asymptotic Eq (1.3.7) improves with time.

Thus, in the case $\gamma>0$, , the gradients blow up like $\frac{1}{a(t)}$ or like "$O(t^{\frac{1}{2\gamma}})$ " as $t\to\infty$. The width of the transition region $r(t)-l(t)$ equal to

$$2\frac{C}{\sqrt{\beta}}a(t)=2\frac{C}{\sqrt{\beta}}\left(2\gamma\beta t+A_0\right)^{\frac{-1}{2\gamma}},$$

which decreases with time. In this case the phenomenon of gradient enhancement takes place: The spatial gradient of the solutions u_x, increases with time, and its support shrinks. See Figures 10, 11.

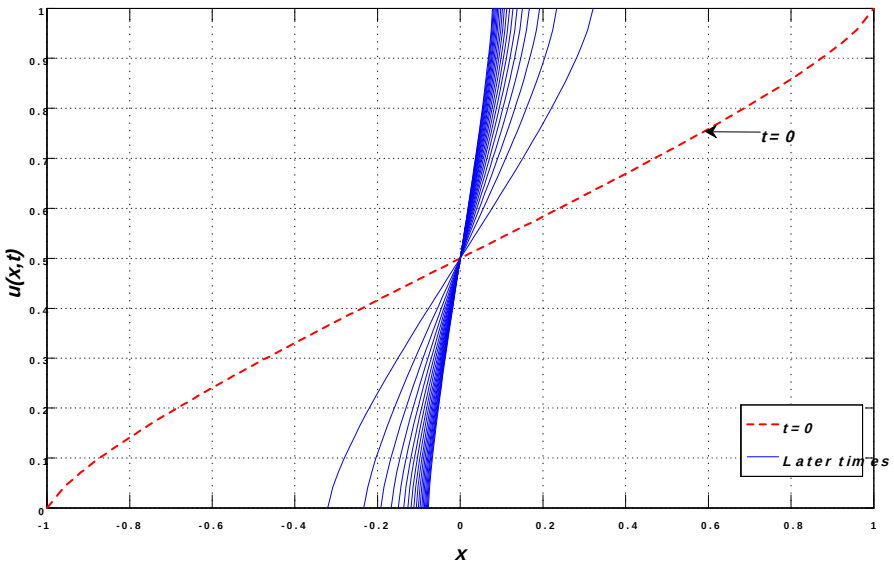

Figure 10: The evolution of the image intensity distribution $u(x,t)$ for $\gamma = \frac{1}{2}$.

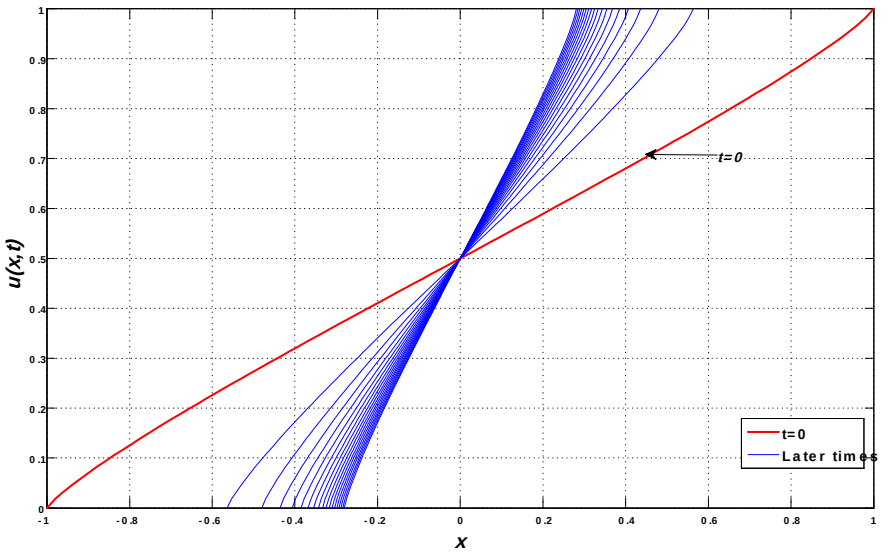

Figure 11: The evolution of the image intensity distribution $u(x,t)$ for $\gamma = 1$. "the Beltrami flow".

2.3.2 Self similar solution of type II

We study now the case $\frac{-1}{2} < \gamma < 0$, when we recover the self similar solution of Type II (2.1.2)-(2.3.8), in this case $a(t)$, is given by:

$$a(t) = (2\gamma\beta t + A_0)^{\frac{-1}{2\gamma}}, \qquad \text{for } 0 < t < T \text{ with } T = -\frac{A_0}{2\gamma\beta}, \text{ and } A_0 > 0. \tag{2.3.17}$$

The profile f is given by (2.3.6), which can be written as

$$\frac{df}{d\xi} = \left[\frac{1}{1+\gamma}\right]^{\frac{1}{2(1+\gamma)}} C^{\frac{-1}{1+\gamma}} \left[1 - \left(\frac{\sqrt{\beta}\xi}{C}\right)^2\right]^{\frac{-1}{2(1+\gamma)}}, \text{ with } \frac{-1}{2} < \gamma < 0, \tag{2.3.18}$$

for

$$-\frac{C}{\sqrt{\beta}} \leq \xi \leq \frac{C}{\sqrt{\beta}}.$$

The solution of (2.3.18) is given as in previous section by

$$f(\xi) = \frac{1}{\sqrt{\beta}} \left[\frac{1}{1+\gamma}\right]^{\frac{1}{2(1+\gamma)}} C^{\frac{\gamma}{1+\gamma}} \int_{-1}^{\frac{\sqrt{\beta}}{C}\xi} \frac{d\eta}{[1-\eta^2]^{\frac{1}{2(1+\gamma)}}}, \tag{2.3.19}$$

for $\frac{-1}{2} < \gamma < 0$, where C is integration constant given by (2.3.14).

Thus, the self similar solutions of the Type II (2.1.2)-(2.3.8), assumes the form

$$u(x,t) = \frac{1}{\sqrt{\beta}} \left[\frac{1}{1+\gamma}\right]^{\frac{1}{2(1+\gamma)}} C^{\frac{\gamma}{1+\gamma}} \int_{-1}^{\frac{\sqrt{\beta}}{C}\frac{x}{a(t)}} \frac{d\eta}{[1-\eta^2]^{\frac{1}{2(1+\gamma)}}}. \tag{2.3.20}$$

With $a(t)$ given by (2.3.8).

The gradients are given by

$$u_x(x,t) = \frac{1}{a(t)} \left[\frac{1}{1+\gamma}\right]^{\frac{1}{2(1+\gamma)}} C^{\frac{-1}{1+\gamma}} \left[1 - \left(\sqrt{\beta}\frac{x}{Ca(t)}\right)^2\right]^{\frac{-1}{2(1+\gamma)}}, \text{ for } \frac{-1}{2} < \gamma < 0. \tag{2.3.21}$$

we can see that if $t \to T$, *then* $u_x(x,t) \to \infty$, (because $a(t) \to 0$) and the validity of the asymptotic Eq (1.3.7) improves with time.

Thus, the gradient blows up like $\frac{1}{a(t)}$ as $t \to T$. The width of the transition region$r(t) - l(t)$ equal to $2\frac{C}{\sqrt{\beta}}\left(2\gamma\beta t + A_0\right)^{\frac{-1}{2\gamma}}$ which decreases with time.

In this case the phenomenon of gradient enhancement takes place: The spatial gradient of the solutions, u_x, increases with time, and its support shrinks. See Figure 12.

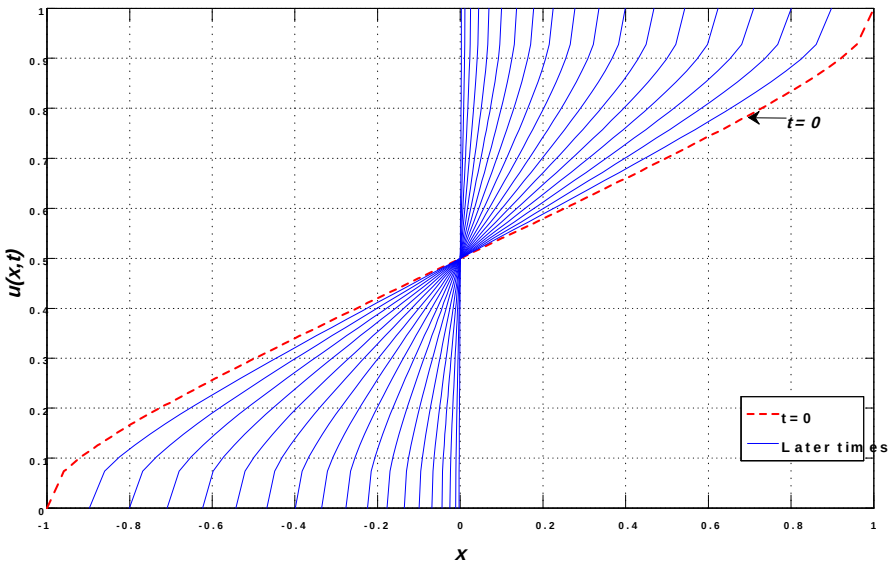

Figure 12: The evolution of the image intensity distribution $u(x,t)$ for $\gamma = \frac{-1}{4}$.

2.3.3 Self similar solution of type III

Now, we descus the particular case $\gamma = 0$, Self-similar solution of third type (2.3.10) is obtained.

In this case, the equation (1.3.7) becomes

$$u_t = u_x^{-2} u_{xx}. \tag{2.3.22}$$

If we replace the solution (2.1.2) in equation (2.3.22), we obtain

$$-\frac{\dot{a}}{a}\xi\frac{df}{d\xi} = \left(\frac{df}{d\xi}\right)^{-2}\frac{d^2 f}{d\xi^2}. \tag{2.3.23}$$

A separation of variables argument implies that the following conditions must hold:

$$\frac{\dot{a}}{a} = -\beta. \tag{2.3.24}$$

The resolution of (2.3.24) gives:

$$a(t) = A_0 e^{-\beta t}, \text{ for } 0 < t < \infty. \tag{2.3.25}$$

The equation for the profile f, becomes:

$$\beta\xi \frac{df}{d\xi} = \left(\frac{df}{d\xi}\right)^{-2} \frac{d^2 f}{d\xi^2},$$

which can be written as

$$\left(\frac{df}{d\xi}\right)^{-3} \frac{d^2 f}{d\xi^2} = \beta\xi. \tag{2.3.26}$$

After integration of (2.3.26), we obtain

$$\frac{df}{d\xi} = \frac{1}{C}\left[1 - \left(\frac{\sqrt{\beta}\xi}{C}\right)^2\right]^{\frac{-1}{2}},$$

where $C > 0$ is an integration constant. By using the boundary conditions $f\left(-\frac{C}{\sqrt{\beta}}\right) = 0$, and $f\left(\frac{C}{\sqrt{\beta}}\right) = 1$, we obtain, after integration:

$$f(\xi) = \frac{1}{\pi}\arcsin\left(\frac{\pi\xi}{C}\right) + \frac{1}{2}; \quad \text{with} \quad \beta = \pi^2, \tag{2.3.27}$$

for

$$-\frac{C}{\pi} \leq \xi \leq \frac{C}{\pi}.$$

Thus, we obtain self similar solutions of the Type III, with the form

$$u(x,t) = \frac{1}{\pi}\arcsin\left(\pi\frac{x}{Ca(t)}\right) + \frac{1}{2}; \tag{2.3.28}$$

for the boundary layer

$$l(t) = -\frac{C}{\pi}a(t) \leq x \leq \frac{C}{\pi}a(t) = r(t),$$

where $a(t)$ is given by (2.3.25).

The gradients are given by

$$u_x(x,t) = \frac{1}{a(t)}\frac{df}{d\xi} = \frac{1}{Ca(t)}\left[1 - \left(\pi\frac{x - x_0}{Ca(t)}\right)^2\right]^{\frac{-1}{2}} \tag{2.3.29}$$

We can see that if $t \to \infty$, we have $u_x(x,t) \to \infty$, $(for\ a(t) \to 0)$.

Thus the gradients blow up exponentially as $t \to \infty$. The width of the transition region $r(t) - l(t)$ is given by $2\frac{C}{\pi}A_0 e^{-\pi^2 t}$ which decreases with time. In this case the phenomenon of edge enhancement takes place for this class of equations ($\gamma = 0$), see Figure 13.

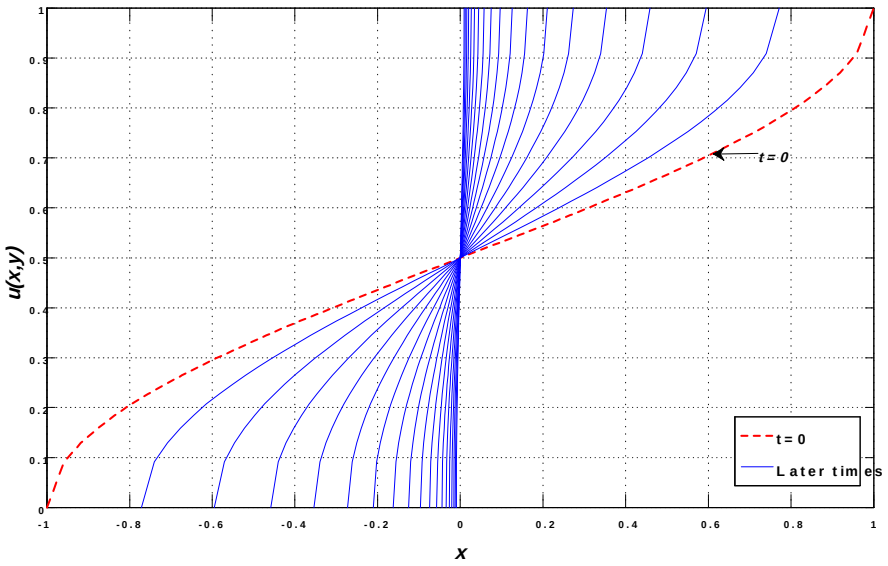

Figure 13: The evolution of the image intensity distribution $u(x,t)$ for $\gamma = 0$.

The case $\alpha = -1$:

The equation (1.3.7) becomes:

$$u_t = u_{xx}.$$

If we replace the solution (2.1.2) in this equation, we obtain

$$-\frac{\dot{a}}{a}\xi\frac{df}{d\xi} = \frac{1}{a^2}\frac{d^2 f}{d\xi^2}.$$

A separation of variables argument implies that the following conditions must hold :

$$\dot{a}a = -\beta,$$

where $\beta < 0$ is arbitrary constant.

Easy integration gives:

$$a(t) = (-2\beta t + A_0)^{\frac{1}{2}}, \quad 0 < t < \infty .$$

The equation for the profile f , becomes:

$$\beta\xi \frac{df}{d\xi} = \frac{d^2 f}{d\xi^2},$$

which can be written as

$$\left(\frac{df}{d\xi}\right)^{-1} \frac{d^2 f}{d\xi^2} = \beta\xi.$$

After integration, we obtain

$$\frac{df}{d\xi} = \exp\left[\frac{1}{2}C^2 - \left(\frac{\sqrt{-\beta}\xi}{\sqrt{2}}\right)^2\right],$$

Here, C is an integration constant. By using the boundary conditions, we obtain the relation for C:

$$C = \left[2\ln\left(\frac{\sqrt{-\beta}}{\sqrt{2}\pi}\right)\right]^{\frac{1}{2}};$$

The profile f is given by:

$$f(\xi) = \frac{1}{\pi}\int_{-\infty}^{\frac{\sqrt{-\beta}\xi}{\sqrt{2}}} e^{-\eta^2} d\eta.$$

Thus, the self similar solution assumes the form

$$u(x,t) = \frac{1}{\pi}\int_{-\infty}^{\sqrt{\frac{-\beta}{2}}\frac{x-x_0}{a(t)}} e^{-\eta^2} d\eta;$$

The gradient is given by

$$u_x(x,t) = \frac{1}{a(t)}\frac{df}{d\xi} = \frac{1}{a(t)}\exp\left[\frac{1}{2}C^2 - \left(\sqrt{\frac{-\beta}{2}}\frac{x-x_0}{a(t)}\right)^2\right].$$

If $t \to \infty$, we have $u_x(x,t) \to 0$, $(for\ a(t) \to \infty)$. This solution demonstrates that for a linear case $(\gamma = -1)$, the width of the transition region increases with time proportionally to $\sqrt{t + A_0}$, and the gradient u_x decreases with time as $\frac{1}{\sqrt{t+A_0}}$.

2.4 Comments and Conclusion

In this chapter we have studied the contour enhancement in image processing, by resolving a free boundary problem for a nonlinear degenerate parabolic equation via general form of self similar solutions. The results obtained are new and generalize the results obtained by G. I Barenblatt and J. L. Vasquez in [3, 4] for enhancement exponent range $\gamma > 0$. We recover three types of self similar solutions which describe contour enhancement in the larger exponent range $\gamma > \frac{-1}{2}$. These solutions are called of type I, II and III.

Actually, we see examples with $\gamma > \frac{-1}{2}$, we do not see the case when $-1 < \gamma < \frac{-1}{2}$, so that it is possible, in principle, that complete enhancement happens whenever $\gamma > -1$. Of course, a better understanding of this arguments is desirable and will be subject of the next chapter.

The case $\gamma = \frac{-1}{2}$ needs to be studied in more depth and will be subject of future studies.

Chapter 3

New exact solutions to nonlinear diffusion equation that occurs in image processing

In this chapter, we, first, propose to find exact solutions to equation (1.3.7) by introducing the "travelling profiles solutions" proposed by benhamidouche et al. [6, 5], to seek exact solutions for some nonlinear partial differential equations. This form is more general than the form proposed in chapter two. We seek solutions in the form:

$$u(x,t) = c(t) f\left(\frac{x - b(t)}{a(t)}\right), \tag{3.0.1}$$

where the coefficients $a(t), b(t), c(t)$ are functions which depend on time t and f is the basic profile, these functions are to be determined.

On the other hand, we present a generalization of the results proposed in [3], and we show that such a behavior can be observed in the larger exponent range $\gamma > -1$, directly by using solutions (3.0.1). We note that this problem has been investigated by Vasquez and Barenblatt in [4] but with complicated conjugate formulation.

This work has been published in *'International Journal of Computing Science and Mathematics'* [11].

3.1 Travelling profiles solutions to nonlinear degenerate parabolic equation

Now, we want to find exact travelling profiles solutions (3.0.1) of nonlinear degenerate equation (1.3.7). The form (3.0.1) is written as follow:

$$u(x,t) = c(t)\, f(\xi), \text{ with } \xi = \frac{x - b(t)}{a(t)}, \quad \text{for } x \in \mathbb{R},\ t > 0, \tag{3.1.1}$$

where the parameters $a(t)$, $c(t)$, $b(t)$ and the profile f should be determined.

If we replace this form of solutions in equation (1.3.7), we obtain:

$$\frac{\dot{c}}{c} f - \frac{\dot{a}}{a}\xi f'_\xi - \frac{\dot{b}}{a} f'_\xi = \frac{c^{-2-2\gamma}}{a^{-2\gamma}} f_\xi^{-2(1+\gamma)} f"_{\xi\xi}. \tag{3.1.2}$$

This equation depends on many unknown parameters and our aim is to determine the coefficients $a(t), c(t), b(t)$ and the profile f. Hence, we use the "travelling profiles method" (TPM) [6, 5].

The principle of TPM is to determine firstly the coefficients $a(t), c(t)$ and $b(t)$ by resolving the following minimization problem:

$$\min_{\dot{c},\dot{a},\dot{b}} \int_{-\infty}^{+\infty} \left| \frac{\partial u}{\partial t} - u_x^{-2(1+\gamma)} u_{xx} \right|^2 dx.$$

So, we obtain three orthogonal equations, as follows:

$$\begin{cases} \langle \frac{\partial u}{\partial t} - u_x^{-2(1+\gamma)} u_{xx}, f \rangle = 0 \\ \langle \frac{\partial u}{\partial t} - u_x^{-2(1+\gamma)} u_{xx}, \xi f_\xi \rangle = 0 \\ \langle \frac{\partial u}{\partial t} - u_x^{-2(1+\gamma)} u_{xx}, f_\xi \rangle = 0 \end{cases}, \tag{3.1.3}$$

where $\langle ., . \rangle$ is the inner product in L^2 space.

Then, the PDE (1.3.7) is transformed into a set of three coupled ODE's:

$$\begin{cases} \frac{\dot{c}}{c}\langle f, f\rangle - \frac{\dot{a}}{a}\langle \xi f_\xi, f\rangle - \frac{\dot{b}}{a}\langle f_\xi, f\rangle = \frac{c^{-2-2\gamma}}{a^{-2\gamma}}\langle f_\xi^{-2(1+\gamma)} f_{\xi\xi}, f\rangle \\ \frac{\dot{c}}{c}\langle \xi f_\xi, f\rangle - \frac{\dot{a}}{a}\langle \xi f_\xi, \xi f_\xi\rangle - \frac{\dot{b}}{a}\langle \xi f_\xi, f_\xi\rangle = \frac{c^{-2-2\gamma}}{a^{-2\gamma}}\langle f_\xi^{-2(1+\gamma)} f_{\xi\xi}, \xi f_\xi\rangle \\ \frac{\dot{c}}{c}\langle f_\xi, f\rangle - \frac{\dot{a}}{a}\langle f_\xi, \xi f_\xi\rangle - \frac{\dot{b}}{a}\langle f_\xi, f_\xi\rangle = \frac{c^{-2-2\gamma}}{a^{-2\gamma}}\langle f_\xi^{-2(1+\gamma)} f_{\xi\xi}, f_\xi\rangle. \end{cases} \tag{3.1.4}$$

To find exact solutions in the form (3.1.1), we based on the following main theorem [11].

Theorem 3.1.1 *For $f \in C^2 \cap L^2$, the equation (1.3.7) admits an exact solution in the form (3.1.1) if:*

1. $u_x^{-2(1+\gamma)} u_{xx} = \frac{c^{-2-2\gamma}}{a^{-2\gamma}} f_\xi^{-2(1+\gamma)} f_{\xi\xi}$.
2. *The basic profile f is a solution of the following differential equation:*

$$f_\xi^{-2(1+\gamma)} f_{\xi\xi} = \alpha f + \beta \xi f_\xi + \lambda f_\xi, \qquad \text{where } \alpha, \beta, \lambda \in \mathbb{R}. \tag{3.1.5}$$

And we distinguish two cases;

***In the first case**, we have two time behaviors of the coefficients $c(t), a(t)$ and $b(t)$. They are given by:*

$$\begin{cases} a(t) = \left[K_0^{-2-2\gamma} S\beta t + A_0\right]^{\frac{-1}{S}} \\ c(t) = K_0 \left[K_0^{-2-2\gamma} S\beta t + A_0\right]^{\frac{\alpha}{\beta S}} \\ b(t) = \frac{\lambda}{\beta} \left[K_0^{-2-2\gamma} S\beta t + A_0\right]^{\frac{-1}{S}} + A_1 \end{cases}, \quad \text{for } 0 < t < T, \text{ and } S\beta < 0, \tag{3.1.6}$$

with

$$T = -\frac{A_0 K_0^{2+2\gamma}}{S\beta}.$$

And

$$\begin{cases} a(t) = \left[K_0^{-2-2\gamma} S\beta t + A_0\right]^{\frac{-1}{S}} \\ c(t) = K_0 \left[K_0^{-2-2\gamma} S\beta t + A_0\right]^{\frac{\alpha}{\beta S}} \\ b(t) = \frac{\lambda}{\beta} \left[K_0^{-2-2\gamma} S\beta t + A_0\right]^{\frac{-1}{S}} + A_1 \end{cases}, \quad \text{for } 0 < t < \infty, \text{ and } S\beta > 0, \tag{3.1.7}$$

with

$$S = \frac{2(1+\gamma)\alpha + 2\gamma\beta}{\beta}, \quad \text{and} \quad A_0 > 0, K_0 > 0, A_1 \text{ are constants.}$$

***In the second case** (for $S = 0$), we have:*

$$\begin{cases} a(t) = A_0 \exp(-K_0^{-2-2\gamma} \beta t) \\ c(t) = K_0 A_0^{-\frac{\alpha}{\beta}} \exp(K_0^{-2-2\gamma} \alpha t) \\ b(t) = \frac{\lambda}{\beta} A_0 \exp(-K_0^{-2-2\gamma} \beta t) + A_1 \end{cases}, \quad \text{for } 0 < t < \infty, \tag{3.1.8}$$

with

$$A_0 > 0, \ K_0 > 0, \ A_1 \text{ are constants.}$$

Proof. Let

$$V_t = \{f, f_\xi, \xi f_\xi, \},$$

the subspace of L^2 generated by associated functions to f at the moment t.

From (3.1.3), we deduce that $\frac{\partial u}{\partial t} - u_x^{-2(1+\gamma)} u_{xx}$ is orthogonal to subspace V_t. Indeed, we have $\frac{\partial u}{\partial t} \in V_t$, then

$$\langle \frac{\partial u}{\partial t} - u_x^{-2(1+\gamma)} u_{xx}, \frac{\partial u}{\partial t} \rangle = 0.$$

Thus, if also $u_x^{-2(1+\gamma)} u_{xx}$ belongs to V_t, then the method provides us a weakly exact solution, which is written under the form:

$$u(x,t) = c(t) f\left[\frac{x - b(t)}{a(t)}\right].$$

According to the principle of this method, if $u_x^{-2(1+\gamma)} u_{xx} = \frac{c^{-2-2\gamma}}{a^{-2\gamma}} f_\xi^{-2(1+\gamma)} f_{\xi\xi}$ belongs to the subspace V_t, then the function (3.1.1) is an exact solution of equation (1.3.7). In this case, the term $f_\xi^{-2(1+\gamma)} f_{\xi\xi}$ can be expressed as a linear combination of functions $f, \xi f_\xi$, and f_ξ; hence,

$$f_\xi^{-2(1+\gamma)} f_{\xi\xi} = \alpha f + \beta \xi f_\xi + \lambda f_\xi, \text{ for } \alpha, \beta, \lambda \in \mathbb{R}.$$

The coefficients $c(t), a(t)$ and $b(t)$ are obtained as follow:

When we replace $f_\xi^{-2(1+\gamma)} f_{\xi\xi}$ by the combination $\alpha f + \beta \xi f_\xi + \lambda f_\xi$ in (3.1.4), we obtain the following system:

$$AX = \frac{c^{-2-2\gamma}}{a^{-2\gamma}} AB, \tag{3.1.9}$$

with

$$A = \begin{pmatrix} \langle f, f\rangle & \langle \xi f_\xi, f\rangle & \langle f_\xi, f\rangle \\ \langle \xi f_\xi, f\rangle & \langle \xi f_\xi, \xi f_\xi\rangle & \langle \xi f_\xi, f_\xi\rangle \\ \langle f_\xi, f\rangle & \langle \xi f_\xi, f_\xi\rangle & \langle f_\xi, f_\xi\rangle \end{pmatrix}, X = \begin{pmatrix} \frac{\dot{c}}{c} \\ -\frac{\dot{a}}{a} \\ -\frac{\dot{b}}{a} \end{pmatrix} \text{ and } B = \begin{pmatrix} \alpha \\ \beta \\ \lambda \end{pmatrix},$$

where $\langle ., . \rangle$ is the inner product in L^2.

The matrix A is symmetric and invertible [6, 5], then the system (3.1.9) can be written as follows:

$$\begin{cases} \frac{\dot{c}}{c} = \alpha \frac{c^{-2-2\gamma}}{a^{-2\gamma}} \\ \frac{\dot{a}}{a} = -\beta \frac{c^{-2-2\gamma}}{a^{-2\gamma}} \\ \frac{\dot{b}}{a} = -\lambda \frac{c^{-2-2\gamma}}{a^{-2\gamma}} \end{cases}. \tag{3.1.10}$$

The resolution of the system (3.1.10) isn't difficult. Indeed, from (3.1.10) we have:

$$\begin{cases} c(t) = K_0 a(t)^{\frac{-\alpha}{\beta}} \\ b(t) = \frac{\lambda}{\beta} a(t) + A_1 \end{cases}, \tag{3.1.11}$$

where $K_0 > 0$ is an integration constant.

If we replace (3.1.11) in (3.1.10) then we deduce (3.1.6),(3.1.7) and (3.1.8). ■

We notice that from this theorem, we have three time behaviors of coefficients $c(t)$, $a(t)$ and $b(t)$, these behaviors depends on parameters of similarity α, β.

3.2 New exact solutions to nonlinear degenerate parabolic equation

In this section, we consider a particular case, when $\alpha = \beta$, this assumption corresponds to physical law (conservation of mass):

$$\int_{\mathbb{R}} u(s,t)\, ds = const, \tag{3.2.1}$$

indeed, from (3.0.1), we have

$$\int_{\mathbb{R}} u(s,t)\, ds = \int_{\mathbb{R}} c(t) f\left(\frac{s - b(t)}{a(t)}\right) ds = a(t) c(t) \int_{\mathbb{R}} f(\xi)\, d\xi = const,$$

this implies that

$$c(t) = \frac{const}{a(t)}, \tag{3.2.2}$$

from relation (3.1.11) and (3.2.2), we can deduce $\alpha = \beta$.

In this case, a new explicit solution is obtained to equation (1.3.7). Indeed, the equation of profile f (3.1.5) becomes:

$$f_\xi^{-2(1+\gamma)} f_{\xi\xi} = [(\alpha\xi + \lambda) f]_\xi, \qquad \text{where } \alpha, \lambda \in \mathbb{R}. \tag{3.2.3}$$

After integration, we obtain:

$$\frac{-1}{2\gamma + 1} f_\xi^{-2\gamma - 1} = (\alpha\xi + \lambda) f + k, \text{ with } k \text{ is constant.}$$

If we put for example $f(0) = f_\xi(0) = 0$, this implies $k = 0$, we obtain:

$$f_\xi^{-2\gamma-1} = -(2\gamma+1)(\alpha\xi+\lambda) f, \tag{3.2.4}$$

this implies,

$$f^{\frac{1}{2\gamma+1}} df = ((2\gamma+1)(-\alpha\xi-\lambda))^{\frac{-1}{2\gamma+1}} d\xi. \tag{3.2.5}$$

After integration, we obtain:

$$\frac{2\gamma+1}{2\gamma+2} f^{\frac{2\gamma+2}{2\gamma+1}} = \frac{(2\gamma+1)^{\frac{2\gamma}{2\gamma+1}}}{-2\alpha\gamma}(-\alpha\xi-\lambda)^{\frac{2\gamma}{2\gamma+1}} + K, \tag{3.2.6}$$

where K is an integration constant.

Then, the solution of (3.2.3) is written under the form:

$$\begin{aligned} f(\xi) = &\left[\frac{(2\gamma+2)(2\gamma+1)^{\frac{1}{2\gamma+1}}}{2\gamma}\right]^{\frac{2\gamma+1}{2\gamma+2}} \times \\ &\left[\left(\frac{-1}{\alpha}\left[(-\alpha\xi-\lambda)_+\right]^{\frac{2\gamma}{2\gamma+1}} + K\right)_+\right]^{\frac{2\gamma+1}{2\gamma+2}}, \quad \text{for} \quad \gamma > 0. \end{aligned} \tag{3.2.7a}$$

Finally, an explicit exact solution to the nonlinear degenerate parabolic equation (1.3.7) is given as follows:

$$\begin{aligned} u(x,t) = c(t)&\left[\frac{(2\gamma+1)^{\frac{2\gamma+2}{2\gamma+1}}}{2\gamma}\right]^{\frac{2\gamma+1}{2\gamma+2}} \times \\ &\left[\left(\frac{-1}{\alpha}\left[(-\alpha\frac{x-b(t)}{a(t)}-\lambda)_+\right]^{\frac{2\gamma}{2\gamma+1}} + K\right)_+\right]^{\frac{2\gamma+1}{2\gamma+2}}, \text{ for } \gamma > 0. \end{aligned} \tag{3.2.8}$$

The coefficients $c(t), a(t)$ and $b(t)$ are given, explicitly, by:

$$\begin{cases} a(t) = \left[K_0^{-2-2\gamma} S\alpha t + A_0\right]^{\frac{-1}{S}} \\ c(t) = K_0\left[K_0^{-2-2\gamma} S\alpha t + A_0\right]^{\frac{1}{S}} \quad , \ \textit{for } 0 < t < T, \ \textit{and} \ \ \beta = \alpha < 0, \\ b(t) = \frac{\lambda}{\alpha}\left[K_0^{-2-2\gamma} S\alpha t + A_0\right]^{\frac{-1}{S}} + A_1 \end{cases} \tag{3.2.9}$$

with

$$T = \frac{-A_0 K_0^{2+2\gamma}}{S\alpha}.$$

And

$$\begin{cases} a(t) = \left[K_0^{-2-2\gamma} S\alpha t + A_0\right]^{\frac{-1}{S}} \\ c(t) = K_0\left[K_0^{-2-2\gamma} S\alpha t + A_0\right]^{\frac{1}{S}} \quad , \ \textit{for } 0 < t < \infty, \ \textit{and } \beta = \alpha > 0, \\ b(t) = \frac{\lambda}{\alpha}\left[K_0^{-2-2\gamma} S\alpha t + A_0\right]^{\frac{-1}{S}} + A_1 \end{cases} \tag{3.2.10}$$

where $S = 2(1+2\gamma) > 2$, for $\gamma > 0$ and $A_0, K_0 > 0$, A_1 are constants.

So, a new explicit solution is obtained.

3.3 Application to contour enhancement in image processing

A particular case in the discussion now when we consider the case $\alpha = 0$, $\beta > 0$, $\lambda \in \mathbb{R}$, this corresponds to the following form of solutions:

$$u(x,t) = c_0 f(\xi), \text{ with } \xi = \frac{x - b(t)}{a(t)}, \tag{3.3.1}$$

with interesting application of these solutions in image processing which generalize the results proposed in [3].

With the form of solutions (3.3.1), we can generalize these results. Indeed, if we replace this form of solutions in (0.0.1), we obtain:

$$-\frac{\dot{a}}{a}\xi f'_\xi - \frac{\dot{b}}{a} f'_\xi = \frac{c_0^{-2-2\gamma}}{a^{-2\gamma}} f_\xi^{-2(1+\gamma)} f_{\xi\xi}. \tag{3.3.2}$$

A separation of variables argument implies that:

$$\begin{cases} \frac{\dot{a}}{a} = -\beta \frac{c_0^{-2-2\gamma}}{a^{-2\gamma}} \\ \frac{\dot{b}}{a} = -\lambda \frac{c_0^{-2-2\gamma}}{a^{-2\gamma}} \end{cases}, \tag{3.3.3}$$

where $\beta > 0$ and λ are arbitrary constants, and $\gamma > \frac{-1}{2}$.

The equation for the profile f (3.3.2) becomes:

$$(\beta\xi + \lambda)\frac{df}{d\xi} = \left(\frac{df}{d\xi}\right)^{-2(1+\gamma)} \frac{d^2 f}{d\xi^2}. \tag{3.3.4}$$

According to different value of parameter γ, we discuss the solutions of (3.3.3) and (3.3.4).

The case: $\gamma > 0$:

The resolution of system (3.3.3) is not difficult, indeed from (3.3.3) we have

$$b(t) = \frac{\lambda}{\beta} a(t) + A_1. \tag{3.3.5}$$

If we replace (3.3.5) in (3.3.3), we get

$$\begin{cases} a(t) = \left(\frac{2\gamma\beta}{c_0^{2(1+\gamma)}} t + A_0 \right)^{\frac{-1}{2\gamma}} \\ b(t) = \frac{\lambda}{\beta} \left(\frac{2\gamma\beta}{c_0^{2(1+\gamma)}} t + A_0 \right)^{\frac{-1}{2\gamma}} + A_1 \end{cases}, \text{ for } 0 < t < \infty, \tag{3.3.6}$$

for $\beta > 0$, and $A_0 > 0$, A_1 are constants.

The equation for the profile f (3.3.4) can be written as:

$$\left(\frac{df}{d\xi} \right)^{-1-2(1+\gamma)} \frac{d^2 f}{d\xi^2} = (\beta\xi + \lambda), \qquad \text{where } \beta > 0 \text{ and } \lambda \in \mathbb{R},$$

after integration, we obtain

$$\frac{-1}{2(1+\gamma)} \left(\frac{df}{d\xi} \right)^{-2(1+\gamma)} = \beta \frac{\xi^2}{2} + \lambda\xi + k, \quad \text{with } k \text{ constant},$$

and another integration gives

$$\frac{df}{d\xi} = \left[\frac{1}{1+\gamma} \right]^{\frac{1}{2(1+\gamma)}} C^{\frac{-1}{1+\gamma}} \left[1 - \left(\frac{\beta\xi + \lambda}{C\sqrt{\beta}} \right)^2 \right]^{\frac{-1}{2(1+\gamma)}}, \tag{3.3.7}$$

for

$$-\frac{\lambda + C\sqrt{\beta}}{\beta} \leq \xi \leq -\frac{\lambda - C\sqrt{\beta}}{\beta}.$$

For $\xi = \frac{x - b(t)}{a(t)}$, this relation suggests a free-boundary problem for determination of the image intensity evolution in the boundary layer $l(t)$ and $r(t)$ such that

$$l(t) = b(t) - \frac{\lambda + C\sqrt{\beta}}{\beta} a(t) \leq x \leq b(t) - \frac{\lambda - C\sqrt{\beta}}{\beta} a(t) = r(t),$$

where $a(t), b(t)$ are given by (3.3.6). If we replace $b(t)$ "given by (3.3.5)" we obtain

$$l(t) = A_1 - \frac{C}{\sqrt{\beta}}a(t) \leq x \leq A_1 + \frac{C}{\sqrt{\beta}}a(t) = r(t).$$

Here, C is an integration constant. Further integration and using the boundary conditions $f\left(-\frac{\lambda+C\sqrt{\beta}}{\beta}\right) = 0$, $f\left(-\frac{\lambda-C\sqrt{\beta}}{\beta}\right) = 1$, then we obtain

$$f(\xi) = \frac{1}{\sqrt{\beta}}\left[\frac{1}{1+\gamma}\right]^{\frac{1}{2(1+\gamma)}} C^{\frac{\gamma}{1+\gamma}} \int_{-1}^{\frac{\beta\xi+\lambda}{C\sqrt{\beta}}} \frac{d\eta}{[1-\eta^2]^{\frac{1}{2(1+\gamma)}}};$$

and

$$C = \left[\frac{2}{\sqrt{\beta}}\left[\frac{1}{1+\gamma}\right]^{\frac{1}{2(1+\gamma)}} \int_0^1 \frac{d\eta}{[1-\eta^2]^{\frac{1}{2(1+\gamma)}}}\right]^{-\frac{\gamma+1}{\gamma}}.$$

Thus, the travelling profiles solutions assumes the form:

$$u(x,t) = c_0\left[\frac{1}{\sqrt{\beta}}\left[\frac{1}{1+\gamma}\right]^{\frac{1}{2(1+\gamma)}} C^{\frac{\gamma}{1+\gamma}} \int_{-1}^{\sqrt{\beta}\frac{x-A_1}{Ca(t)}} \frac{d\eta}{[1-\eta^2]^{\frac{1}{2(1+\gamma)}}}\right].$$

The gradients are given by

$$u_x(x,t) = \frac{c_0}{a(t)}f'(\xi),$$

from (3.3.7), we have

$$u_x(x,t) = \frac{c_0}{a(t)}\left[\frac{1}{1+\gamma}\right]^{\frac{1}{2(1+\gamma)}} C^{\frac{-1}{1+\gamma}}\left[1-\left(\sqrt{\beta}\frac{x-A_1}{Ca(t)}\right)^2\right]^{\frac{-1}{2(1+\gamma)}}.$$

$$if \quad t \to \infty, \ then \quad u_x(x,t) \to \infty, \quad (a(t) \to 0).$$

Therefore the validity of the asymptotic equation (1.3.7) improves with time. Thus, the gradients blow up like $\frac{1}{a(t)}$ or like "$O(t^{\frac{1}{2\gamma}})$ " as $t \to \infty$. The width of the transition region $r(t) - l(t)$ equal to $2\frac{C}{\sqrt{\beta}}a(t) = 2\frac{C}{\sqrt{\beta}}\left(\frac{2\gamma\beta}{c_0^{2(1+\gamma)}}t + A_0\right)^{\frac{-1}{2\gamma}}$ decreases with time.

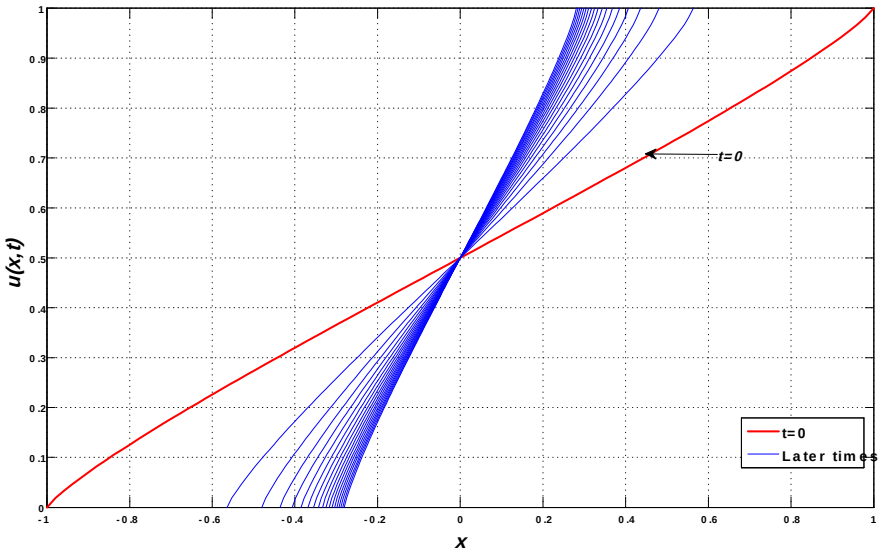

Figure 14: The evolution of the image intensity distribution $u(x,t)$ for $\gamma = 2$.

In this case the phenomenon of gradient enhancement takes place: The spatial gradient of the solutions, u_x, increases with time, and its support shrinks. See figures 14, 15, 16.

REMARK: The particular case when we take in (1.3.7), $c(t)$ and $b(t)$ are constants,then, for $\beta = \frac{1}{2\gamma}$, and $A_0 = t_0$, we recover the form of solutions proposed in [3], called "intermediate asymptotic solution" which has been used to analyze the contour enhancement of image intensity $u\,(x,t)$ in image processing.

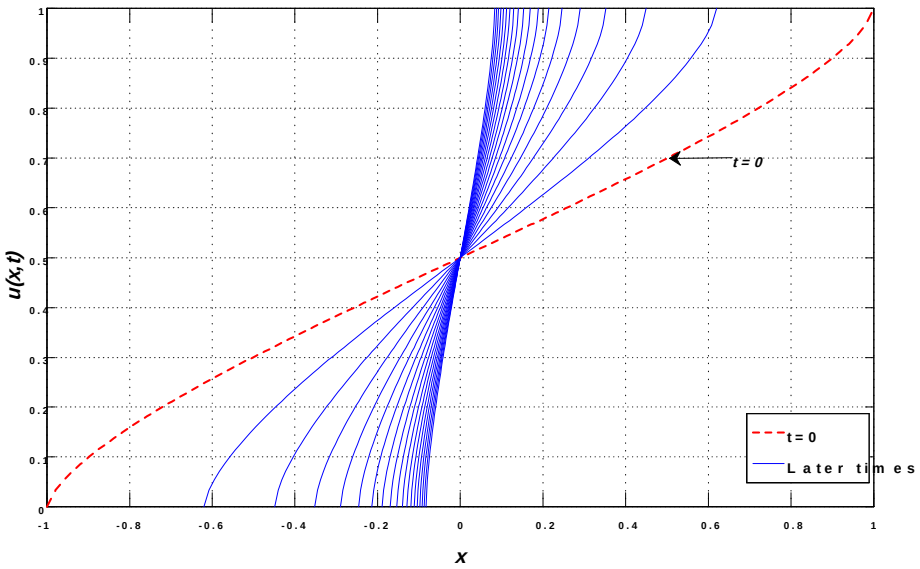

Figure 15: The evolution of the image intensity distribution $u(x,t)$ for $\gamma = 1$.

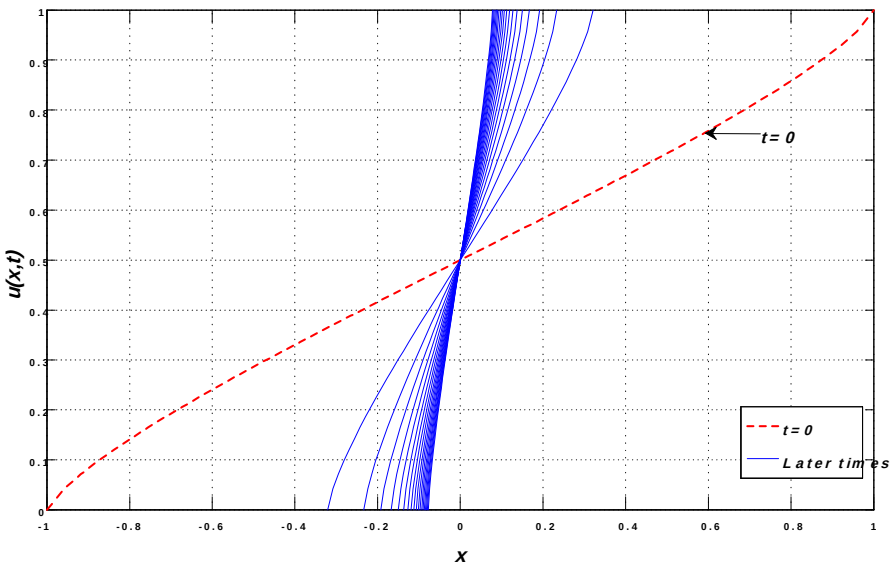

Figure 16: The evolution of the image intensity distribution $u(x,t)$ for $\gamma = \frac{1}{2}$.

The case: $\gamma = 0$:

The equation (1.3.7) becomes:

$$u_t = u_x^{-2} u_{xx}. \tag{3.3.8}$$

If we replace the solution (3.3.1) in equation (3.3.8), we obtain

$$-\frac{\dot{a}}{a}\xi f'_\xi - \frac{\dot{b}}{a}f'_\xi = c_0^{-2} f_\xi^{-2} f_{\xi\xi}. \tag{3.3.9}$$

A separation of variables argument implies that the following conditions must hold :

$$\begin{cases} \frac{\dot{a}}{a} = -\beta c_0^{-2} \\ \frac{\dot{b}}{a} = -\lambda c_0^{-2} \end{cases}, \tag{3.3.10}$$

where β, λ are arbitrary constants .

The resolution of system (3.3.10) gives:

$$\begin{cases} a(t) = A_0 e^{-\beta c_0^{-2} t} \\ b(t) = \frac{\lambda}{\beta} A_0 e^{-\beta c_0^{-2} t} + A_1 \end{cases}, \ for \ \ 0 < t < \infty. \tag{3.3.11}$$

The equation for the profile f becomes:

$$(\beta\xi + \lambda)\frac{df}{d\xi} = \left(\frac{df}{d\xi}\right)^{-2}\frac{d^2 f}{d\xi^2}, \tag{3.3.12}$$

which can be written as

$$\left(\frac{df}{d\xi}\right)^{-3}\frac{d^2 f}{d\xi^2} = (\beta\xi + \lambda), \qquad \text{where } \beta \in \mathbb{R}_+^*, \lambda \in \mathbb{R},$$

after integration, we obtain

$$\frac{df}{d\xi} = \frac{1}{C}\left[1 - \left(\frac{\beta\xi + \lambda}{C\sqrt{\beta}}\right)^2\right]^{\frac{-1}{2}},$$

where $C > 0$ is an integration constant. By using the boundary conditions $f\left(-\frac{\lambda + C\sqrt{\beta}}{\beta}\right) = 0$, and $f\left(-\frac{\lambda - C\sqrt{\beta}}{\beta}\right) = 1$, we obtain, after integration:

$$f(\xi) = \frac{1}{\pi}\arcsin\left(\frac{\pi^2\xi + \lambda}{\pi C}\right) + \frac{1}{2}; \quad \beta = \pi^2,$$

for

$$\frac{-C\pi - \lambda}{\pi^2} \leq \xi \leq \frac{C\pi - \lambda}{\pi^2}.$$

Thus, the travelling profiles solutions assumes the form

$$u\left(x,t\right)=c_0\left[\frac{1}{\pi}\arcsin\left(\pi\frac{x-A_1}{Ca(t)}\right)+\frac{1}{2}\right];$$

for

$$l(t)=b(t)-\frac{\lambda+C\pi}{\pi^2}a(t)\leq x\leq b(t)-\frac{\lambda-C\pi}{\pi^2}a(t)=r(t),$$

where $a(t)$ and $b(t)$ are given by (3.3.11). We can write:

$$l(t)=A_1-\frac{C}{\pi}a(t)\leq x\leq A_1+\frac{C}{\pi}a(t)=r(t).$$

The gradients are given by

$$u_x(x,t)=\frac{c_0}{a(t)}f'(\xi)=\frac{c_0}{Ca(t)}\left[1-\left(\pi\frac{x-A_1}{Ca(t)}\right)^2\right]^{\frac{-1}{2}}.$$

$$\text{if}\quad t\to\infty,\ \text{we have}\ \ u_x(x,t)\to\infty,\ \ (for\ a(t)\to 0).$$

Thus; The gradients blow up exponentially as $t\to\infty$. The width of the transition region $r(t)-l(t)$ is given by $2\frac{C}{\pi}A_0e^{-\left(\frac{\pi}{c_0}\right)^2t}$ decreases with time. In this case the phenomenon of edge enhancement takes place for this class of equations ($\gamma=0$), see figure 17.

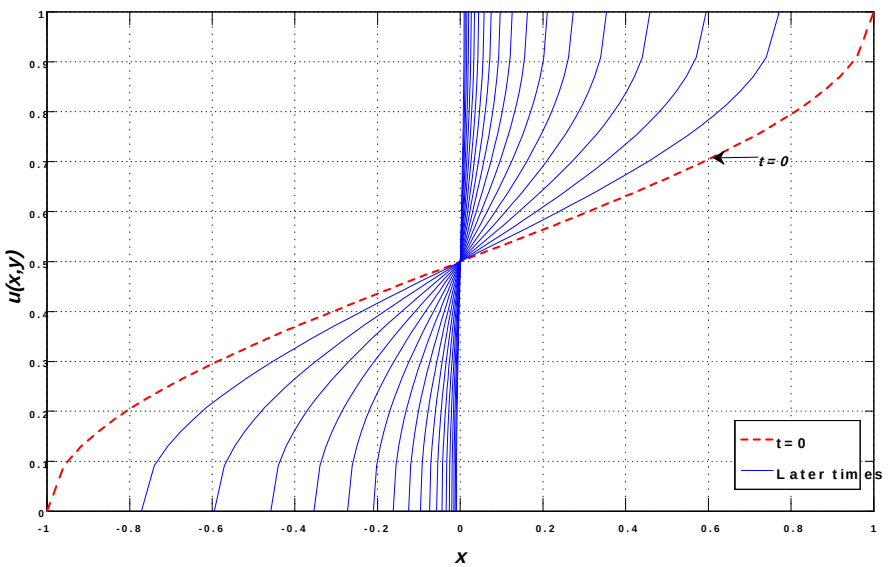

Figure 17: The evolution of the image intensity distribution $u(x,t)$ for $\gamma=0$.

The case: $-1 < \gamma < \frac{-1}{2}$ and $\frac{-1}{2} < \gamma < 0$:

In this case, the parameters $a(t)$ and $b(t)$ are given from (3.3.3) by :

$$\begin{cases} a(t) = \left(\frac{2\gamma\beta}{c_0^{2(1+\gamma)}}t + A_0\right)^{\frac{-1}{2\gamma}} \\ b(t) = \frac{\lambda}{\beta}\left(\frac{2\gamma\beta}{c_0^{2(1+\gamma)}}t + A_0\right)^{\frac{-1}{2\gamma}} + A_1 \end{cases}, \quad 0 < t < T = -\frac{A_0 c_0^{2(1+\gamma)}}{2\gamma\beta}, \tag{3.3.13}$$

with $-1 < \gamma < \frac{-1}{2}$ and $\frac{-1}{2} < \gamma < 0$, and $\beta > 0$, where $A_0 > 0$, A_1 are a constants.

The solution of equation for the profile f (3.3.4), is given by:

$$f(\xi) = \frac{1}{\sqrt{\beta}}\left[\frac{1}{1+\gamma}\right]^{\frac{1}{2(1+\gamma)}} C^{\frac{\gamma}{1+\gamma}} \int_{-1}^{\frac{\beta\xi+\lambda}{C\sqrt{\beta}}} \frac{d\eta}{[1-\eta^2]^{\frac{1}{2(1+\gamma)}}};$$

with

$$\frac{-C\sqrt{\beta}-\lambda}{\beta} \leq \xi \leq \frac{C\sqrt{\beta}-\lambda}{\beta}.$$

The relation for C is given also by:

$$C = \left[\frac{2}{\sqrt{\beta}}\left[\frac{1}{1+\gamma}\right]^{\frac{1}{2(1+\gamma)}} \int_0^1 \frac{d\eta}{[1-\eta^2]^{\frac{1}{2(1+\gamma)}}}\right]^{-\frac{\gamma+1}{\gamma}}.$$

Returning to the variables x and t we obtain the travelling profiles solutions as follow:

$$u(x,t) = c_0\left[\frac{1}{\sqrt{\beta}}\left[\frac{1}{1+\gamma}\right]^{\frac{1}{2(1+\gamma)}} C^{\frac{\gamma}{1+\gamma}} \int_{-1}^{\sqrt{\beta}\frac{x-A_1}{Ca(t)}} \frac{d\eta}{[1-\eta^2]^{\frac{1}{2(1+\gamma)}}}\right],$$

for free boundaries:

$$l(t) = b(t) - \frac{\lambda + C\sqrt{\beta}}{\beta}a(t) \leq x \leq b(t) - \frac{\lambda - C\sqrt{\beta}}{\beta}a(t) = r(t),$$

where $a(t), b(t)$ are given by (3.3.13). We can simply write:

$$l(t) = A_1 - \frac{C}{\sqrt{\beta}}a(t) \leq x \leq A_1 + \frac{C}{\sqrt{\beta}}a(t) = r(t).$$

The gradients are given by

$$\begin{aligned} u_x(x,t) &= \frac{c_0}{a(t)} f'(\xi) \\ &= \frac{c_0}{a(t)} \left[\frac{1}{1+\gamma}\right]^{\frac{1}{2(1+\gamma)}} C^{\frac{-1}{1+\gamma}} \left[1 - \left(\sqrt{\beta}\frac{x-A_1}{Ca(t)}\right)^2\right]^{\frac{-1}{2(1+\gamma)}} . \end{aligned}$$

In this case $lim\ a(t) = 0$, if $t \to T$, then we have:

$$u_x(x,t) \to \infty, \text{ for } t \to T.$$

Therefore the validity of the asymptotic equation (1.3.7) improves with time: The gradients blow up like $\left(\frac{2\gamma\beta}{c_0^{2(1+\gamma)}}t + A_0\right)^{\frac{1}{2\gamma}}$ or like "$O((T-t)^{\frac{1}{2\gamma}})$ " as $t \to T$ The width of the transition region $r(t) - l(t)$ is given by $2\frac{C}{\sqrt{\beta}}\left(\frac{2\gamma\beta}{c_0^{2(1+\gamma)}}t + A_0\right)^{\frac{-1}{2\gamma}}$ decreases with time for $0 < t < T$. See figures 18, 19.

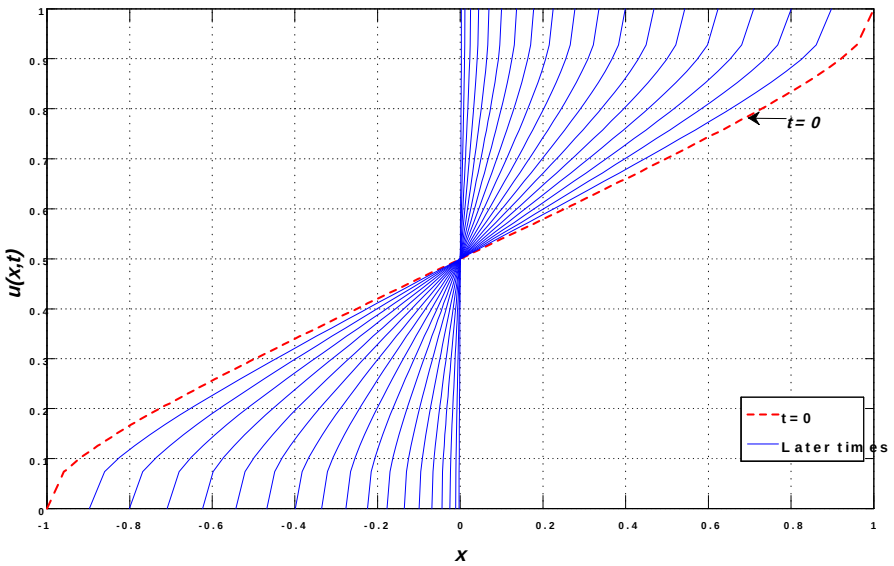

Figure 18: The evolution of the image intensity distribution $u(x,t)$ for $\gamma = \frac{-1}{4}$.

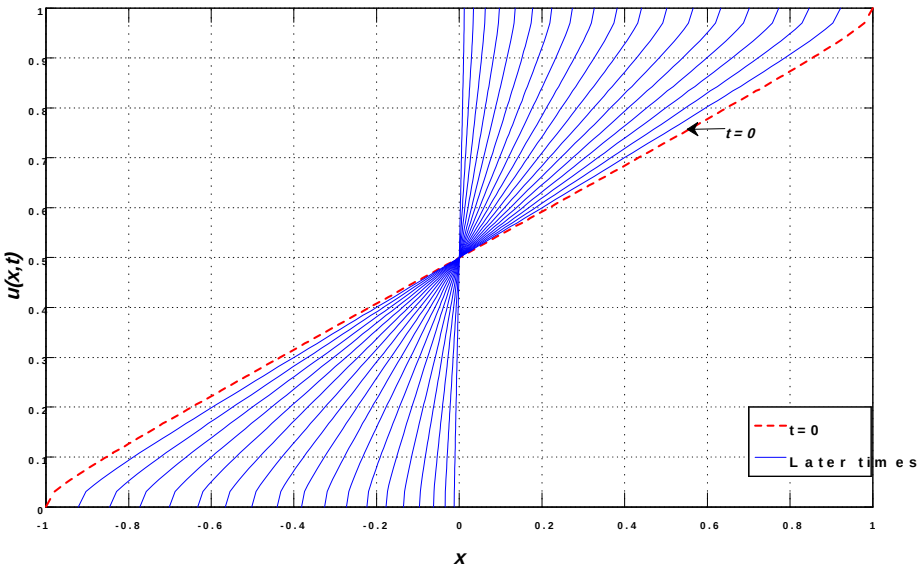

Figure 19: The evolution of the image intensity distribution $u(x,t)$ for $\gamma = \frac{-2}{3}$.

3.4 Comments and Conclusion

In this chapter, we have found new exact solutions of nonlinear diffusion equation (1.3.7) called nonlinear degenerate parabolic equation that occurs in image processing. We have introduced a general form of self similar solutions, called "travelling profiles solutions". We have also given a generalize results obtained for a free boundary problem investigated by Barenblatt [3], to study the contour enhancement in image processing. We have obtained new results in the larger exponent range of parameter enhancement $\gamma > \frac{-1}{2}$, and $-1 < \gamma < \frac{-1}{2}$.

If we examine these new solutions (3.0.1), we note that:

- The case $\alpha = \beta < 0$ shows that the solution (3.2.8) exists locally in time, because the parameters $a(t)$, $c(t)$ and $b(t)$ exist locally in time, exactly for $0 < t < T = \frac{-A_0 K_0^{2+2\gamma}}{S\alpha}$, and can blow up at the time T.

- For the case $\alpha = \beta > 0$, the solution (3.2.8) exists for all time $0 < t < \infty$, because $a(t)$, $c(t)$ and $b(t)$ exist also for all time $0 < t < \infty$.

- We have also given a generalized result obtained for a free boundary problem investigated by Barenblatt [3], to study the contour enhancement in image processing. We have obtained new results in the larger exponent range of parameter enhancement $\gamma > \frac{-1}{2}$, and $-1 < \gamma < \frac{-1}{2}$.

- The general form of solution (3.0.1) can be explored with future work in image processing where the role of the parameters $a(t)$, $c(t)$ and $b(t)$ can be demonstrated in this process.

Chapter 4

Fractional diffusion equation and contour enhancement

The classical calculus provides a powerful tool to model and explains many important dynamically processes in most parts of applied areas of the sciences. But there are many complex systems in nature with anomalous dynamics, including biology, chemistry, physics, geology, astrophysics and social sciences, and more particularly in transport of chemical contaminant through water around rocks, dynamics of viscoelastic materials as polymers, signals theory, control theory, electromagnetic theory, and many more their dynamics can not be characterized by classical derivative models. (for detail [12, 14, 15, 18, 26, 29]).

Fractional calculus is one of the generalizations of the classical calculus and it has been used successfully in various fields of science and engineering.

Indeed, there are new possibilities in mathematics and theoretical physics appear when the order of the differential operator or the integral operator becomes an arbitrary parameter. The fractional calculus is a powerful tool to describe physical systems that have long-term memory and long-range spatial interactions (see [14, 15, 18, 26, 22, 27]).

The derivative of non-integer order has been an interesting research topic for several centuries. The idea was motivated by the question, "What does it mean by $\frac{d^n f}{dx^n}$, if $n = \frac{1}{2}$?", asked by L'Hospital in 1695 in his letters to Leibniz [20]. Since then, the mathematicians

tried to answer this question for centuries in several points of view. The outcomes have many folds. Various types of fractional derivatives were introduced: Riemann-Liouville, Caputo, Hadamard, Erdélyi-Kober, Grünwald-Letnikov, Marchaud and Riesz are just a few to name [16, 17, 24, 26]. Most of the fractional derivatives are defined via fractional integrals [27].

In this chapter, we present new exact solutions of form (3.0.1) for the following fractional diffusion equation

$$D^{\rho}u = u_x^{-2(1+\gamma)}u_{xx}. \tag{4.1}$$

where D^{ρ} denote the fractional derivative of order ρ, and $\rho \in (0,1]$.

4.1 Fractional derivative and classical properties

Among the inconsistencies of the existing fractional derivatives are:

(1) Most of the fractional derivatives except Caputo-type derivatives, do not satisfy $D_a^{\rho}(1) = 0$, if ρ is not a natural number.

(2) All fractional derivatives do not obey the familiar Product Rule for two functions:

$$D^{\rho}(fg) = fD^{\rho}(g) + gD^{\rho}(f).$$

(3) All fractional derivatives do not obey the familiar Quotient Rule for two functions:

$$D^{\rho}(\frac{f}{g}) = \frac{gD^{\rho}(f) - fD^{\rho}(g)}{g^2}.$$

(4) All fractional derivatives do not obey the Chain Rule:

$$D^{\rho}(fog)(t) = f^{(\rho)}(g(t))g^{(\rho)}(t).$$

(5) Fractional derivatives do not have a corresponding Rolle's Theorem.

(6) Fractional derivatives do not have a corresponding Mean Value Theorem.

(7) All fractional derivatives do not obey: $D_a^{\rho}D_a^{\varpi}f = D_a^{\rho+\varpi}f$, in general.

(8) The Caputo definition assumes that the function f is differentiable.

To overcome some of these and other difficulties, Khalil et al. [17], came up with an interesting idea that extends the familiar limit definition of the derivative of a function and interesting properties proved.

Definition 4.1.1 *[17] Let $f : [0, \infty) \to \mathbb{R}$ and $t > 0$. Then the fractional derivative of f of order ρ is defined by:*

$$D^{\rho}(f)(t) = \lim_{\epsilon \to 0} \frac{f(t + \epsilon t^{1-\rho}) - f(t)}{\epsilon},$$

for $t > 0, \rho \in (0, 1)$. If f is $\rho-$differentiable in some $(0, a), a > 0$, and $\lim_{t \to 0^+} D^{\rho}(f)(t)$ exists, then define

$$D^{\rho}(f)(0) = \lim_{t \to 0^+} D^{\rho}(f)(t)$$

Theorem 4.1.1 *[17]If a function $f : [0, \infty) \to \mathbb{R}$ is $\rho-$differentiable at $t_0 > 0$, $\rho \in (0, 1]$, then f is continuous at t_0.*

Proof. [17]Since

$$f(t_0 + \epsilon t_0^{1-\rho}) - f(t_0) = \frac{f(t_0 + \epsilon t_0^{1-\rho}) - f(t_0)}{\epsilon} \epsilon,$$

we have

$$\lim_{\epsilon \to 0} \left[f(t_0 + \epsilon t_0^{1-\rho}) - f(t_0) \right] = \lim_{\epsilon \to 0} \frac{f(t_0 + \epsilon t_0^{1-\rho}) - f(t_0)}{\epsilon} . \lim_{\epsilon \to 0} \epsilon.$$

Let $h = \epsilon t_0^{1-\rho} + O(\epsilon^2)$. Then,

$$\lim_{h \to 0} [f(t_0 + h) - f(t_0)] = D^{\rho}(f)(t_0).0 = 0,$$

which, in turn, implies that

$$\lim_{h \to 0} f(a + h) = f(a).$$

■

One can easily show that D^{ρ} satisfies all the properties in the following theorem.

Theorem 4.1.2 *[17]Let $\rho \in (0,1]$ and f, g be $\rho-$differentiable at a point $t > 0$. Then,*

1. $D^\rho[af + bg] = aD^\rho(f) + bD^\rho(g)$, *for all* $a, b \in \mathbb{R}$.
2. $D^\rho(t^n) = nt^{n-\rho}$, *for all* $n \in \mathbb{R}$.
3. $D^\rho(C) = 0$, *for all constant functions,* $f(t) = C$.
4. $D^\rho(fg) = fD^\rho(g) + gD^\rho(f)$.
5. $D^\rho(\frac{f}{g}) = \frac{gD^\rho(f) - fD^\rho(g)}{g^2}$.
6. $D^\rho(fog)(t) = f'(g(t))D^\rho g(t)$, *for* f *differentiable at* $g(t)$.
7. *If, in addition,* f *is differentiable, then* $D^\rho(f)(t) = t^{1-\rho}\frac{df}{dt}(t)$.

Remark 4.1.1 *The result (6) does not appear in [17].*

Proof. [17]Part (1) and (3) follow directly from the definition. We shall prove (2) For fixed $\rho \in (0,1], n \in \mathbb{R}$ and $t > 0$, we have

$$\begin{aligned} D^\rho(t^n) &= \lim_{\epsilon\to 0} \frac{(t+\epsilon t^{1-\rho})^n - t^n}{\epsilon} \\ &= t^n \lim_{\epsilon\to 0} \frac{(1+\epsilon t^{-\rho})^n - 1}{\epsilon} \\ &= t^n \lim_{\epsilon\to 0} \frac{\epsilon n t^{-\rho} + \frac{\epsilon^2 n(n-1)t^{-2\rho}}{2!} + ...}{\epsilon} \\ &= t^n \lim_{\epsilon\to 0} \frac{n\epsilon t^{-\rho} + O(\epsilon^2)}{\epsilon} \\ &= nt^{n-\rho}. \end{aligned}$$

This completes the proof of (2). Then, we shall prove (4). To this end, since f and g are $\rho - differentiable$ at $t > 0$, note that,

$$\begin{aligned} D^\rho(fg)(t) &= \lim_{\epsilon\to 0} \frac{f(t+\epsilon t^{1-\rho})g(t+\epsilon t^{1-\rho}) - f(t)g(t)}{\epsilon} \\ &= \lim_{\epsilon\to 0} \frac{f(t+\epsilon t^{1-\rho})g(t+\epsilon t^{1-\rho}) - f(t)g(t+\epsilon t^{1-\rho}) + f(t)g(t+\epsilon t^{1-\rho}) - f(t)g(t)}{\epsilon} \\ &= \lim_{\epsilon\to 0} \left[\frac{f(t+\epsilon t^{1-\rho}) - f(t)}{\epsilon}.g(t+\epsilon t^{1-\rho})\right] + f(t)\lim_{\epsilon\to 0}\frac{g(t+\epsilon t^{1-\rho}) - g(t)}{\epsilon} \\ &= D^\rho(f)(t)\lim_{\epsilon\to 0} g(t+\epsilon t^{1-\rho}) + f(t)D^\rho(g)(t). \end{aligned}$$

Since g is continuous at t, $\lim_{\epsilon\to 0} g(t+\epsilon t^{1-\rho}) = g(t)$. This completes the proof of (4). The proof of (5) is similar.

Now, we prove (6) following a standard limit-approach. To this end, in one hand, if the function g is constant in a neighborhood containing t, then $D^\rho(fog)(t) = 0$. On the other hand, assume that the function g is non-constant in the neighborhood of t. In this case, we can find an $\epsilon_0 > 0$ such that, $g(x_1) \neq g(x_2)$ for any $x_1, x_2 \in (t-\epsilon_0, t+\epsilon_0)$. Now, since g is continuous at t, for ϵ sufficiently small, we have

$$\begin{aligned}
D^\rho(fog)(t) &= \lim_{\epsilon\to 0} \frac{f\left(g\left(t+\epsilon t^{1-\rho}\right)\right) - f\left(g\left(t\right)\right)}{\epsilon} \\
&= \lim_{\epsilon\to 0} \frac{f\left(g\left(t+\epsilon t^{1-\rho}\right)\right) - f\left(g\left(t\right)\right)}{g\left(t+\epsilon t^{1-\rho}\right) - g\left(t\right)} . \frac{g\left(t+\epsilon t^{1-\rho}\right) - g\left(t\right)}{\epsilon} \\
&= \lim_{\epsilon\to 0} \frac{f\left(g\left(t\right)+\epsilon_1\right) - f\left(g\left(t\right)\right)}{\epsilon_1} . \frac{g\left(t+\epsilon t^{1-\rho}\right) - g\left(t\right)}{\epsilon}, \quad \text{where } \epsilon_1 \to 0 \text{ as } \epsilon \to 0, \\
&= \lim_{\epsilon_1\to 0} \frac{f\left(g\left(t\right)+\epsilon_1\right) - f\left(g\left(t\right)\right)}{\epsilon_1} . \lim_{\epsilon\to 0} \frac{g\left(t+\epsilon t^{1-\rho}\right) - g\left(t\right)}{\epsilon} \\
&= f'(g(t)) D^\rho g(t),
\end{aligned}$$

for $t > 0$. This establishes the Chain Rule.

To prove part (7), let $h = \epsilon t^{1-\rho}$, then $\epsilon = h t^{\rho-1}$. Therefore,

$$\begin{aligned}
D^\rho(f)(t) &= \lim_{\epsilon\to 0} \frac{f(t+\epsilon t^{1-\rho}) - f(t)}{\epsilon} \\
&= \lim_{h\to 0} \frac{f(t+h) - f(t)}{h t^{\rho-1}} \\
&= t^{1-\rho} \lim_{h\to 0} \frac{f(t+h)) - f(t)}{h} \\
&= t^{1-\rho} \frac{df}{dt}(t)
\end{aligned}$$

■

4.2 Exact solutions to fractional nonlinear diffusion equation

Now, we want to find exact travelling profiles solutions (3.0.1) of fractional nonlinear diffusion equation (4.1).

If we apply the theorem 4.3, we can find:

$$\begin{cases} D_t^{\rho} u(x,t) = t^{1-\rho}\left[\dot{c}f - c\frac{\dot{a}}{a}\xi f'_{\xi} - c\frac{\dot{b}}{a}f'_{\xi}\right] \\ u_x = \frac{c}{a}f' \\ u_{xx} = \frac{c}{a^2}f" \end{cases}$$

Substituting the form (3.0.1) into equation (4.1), we obtain:

$$\frac{\dot{c}}{c}f - \frac{\dot{a}}{a}\xi f'_{\xi} - \frac{\dot{b}}{a}f'_{\xi} = t^{\rho-1}\frac{c^{-2-2\gamma}}{a^{-2\gamma}}f_{\xi}^{-2(1+\gamma)}f_{\xi\xi}, \tag{4.2.1}$$

A simple separation of variables argument implies that the following conditions must hold :

$$\begin{cases} \frac{\dot{c}}{c} = \alpha\frac{c^{-2-2\gamma}}{a^{-2\gamma}}t^{\rho-1} \\ \frac{\dot{a}}{a} = -\beta\frac{c^{-2-2\gamma}}{a^{-2\gamma}}t^{\rho-1} \\ \frac{\dot{b}}{a} = -\lambda\frac{c^{-2-2\gamma}}{a^{-2\gamma}}t^{\rho-1} \end{cases}; \tag{4.2.2}$$

with parameters $\alpha, \beta, \lambda \in \mathbb{R}$, and the basic profile f must satisfy the following ordinary differential equation in ξ:

$$f_{\xi}^{-2(1+\gamma)}f_{\xi\xi} = \alpha f + \beta\xi f'_{\xi} + \lambda f'_{\xi}, \qquad \text{where } \alpha, \beta, \lambda \in \mathbb{R}, \tag{4.2.3}$$

We have to solve system (4.2.2) to find the coefficients $c(t), a(t)$ and $b(t)$. Indeed, from (4.2.2) we have:

$$\begin{cases} c(t) = K_0 a(t)^{\frac{-\alpha}{\beta}} \\ b(t) = \frac{\lambda}{\beta}a(t) + A_1 \end{cases}; \tag{4.2.4}$$

where $K_0 > 0, A_1$ are integration constants. Inserting (4.2.4) into (4.2.2), we get:

(i) **In the first case**, we have two time behaviors of the coefficients $c(t), a(t)$ and $b(t)$. They are given by:

$$\begin{cases} a(t) = \left[K_0^{-2-2\gamma}\frac{S\beta}{\rho}t^{\rho} + A_0\right]^{\frac{-1}{S}} \\ c(t) = K_0\left[K_0^{-2-2\gamma}\frac{S\beta}{\rho}t^{\rho} + A_0\right]^{\frac{\alpha}{\beta S}} \\ b(t) = \frac{\lambda}{\beta}\left[K_0^{-2-2\gamma}\frac{S\beta}{\rho}t^{\rho} + A_0\right]^{\frac{-1}{S}} + A_1 \end{cases}, \quad \text{for } 0 < t < T, \text{ for } S\beta < 0, \tag{4.2.5}$$

with

$$T = \left[-\frac{\rho A_0 K_0^{2+2\gamma}}{S\beta} \right]^{\frac{1}{\rho}},$$

and

$$\begin{cases} a(t) = \left[K_0^{-2-2\gamma} \frac{S\beta}{\rho} t^\rho + A_0 \right]^{\frac{-1}{S}} \\ c(t) = K_0 \left[K_0^{-2-2\gamma} \frac{S\beta}{\rho} t^\rho + A_0 \right]^{\frac{\alpha}{\beta S}} \\ b(t) = \frac{\lambda}{\beta} \left[K_0^{-2-2\gamma} \frac{S\beta}{\rho} t^\rho + A_0 \right]^{\frac{-1}{S}} + A_1 \end{cases}, \quad \text{for } 0 < t < \infty, \text{for } S\beta > 0, \tag{4.2.6}$$

with

$$S = \frac{2(1+\gamma)\alpha + 2\gamma\beta}{\beta}, \quad \text{and} \quad A_0 > 0,\ K_0 > 0,\ A_1 \text{ are constants.}$$

(ii) **In the second case** (for $S = 0$), we have:

$$\begin{cases} a(t) = A_0 \exp(-K_0^{-2-2\gamma} \frac{\beta}{\rho} t^\rho) \\ c(t) = K_0 A_0^{-\frac{\alpha}{\beta}} \exp(K_0^{-2-2\gamma} \frac{\alpha}{\rho} t^\rho) \\ b(t) = \frac{\lambda}{\beta} A_0 \exp(-K_0^{-2-2\gamma} \frac{\beta}{\rho} t^\rho) + A_1 \end{cases}, \quad \text{for } 0 < t < \infty, \tag{4.2.7}$$

with $A_0 > 0$, $K_0 > 0$, A_1 are constants.

We have three time behaviors of coefficients $c(t), a(t)$ and $b(t)$, these behaviors depends on parameters of similarity α and β.

4.3 Some explicit exact solutions

We consider now two interesting particular cases according to the values of α, β and λ, and we seek new exact solutions of (4.1), we show also the asymptotic behaviors of the solutions obtained.

Case1: $\alpha = 0,\ \beta \in \mathbb{R}_+^*,\ \lambda \in \mathbb{R}$:

A particular case in the discussion now when we consider the case $\alpha = 0$, $\beta \in \mathbb{R}_+^*$, $\lambda \in \mathbb{R}$, this corresponds to the following form of solutions:

$$u\left(x,t\right)=c_0 f(\xi),\ \text{with}\ \xi=\frac{x-b(t)}{a\left(t\right)}, \tag{4.3.1}$$

with interesting application of these solutions in image processing which generalize the results proposed in [3].

Indeed, if we replace this form of solutions in (4.1), we obtain:

$$-\frac{\dot{a}}{a}\xi f'_{\xi}-\frac{\dot{b}}{a}f'_{\xi}=\frac{c_0^{-2-2\gamma}}{a^{-2\gamma}}f_{\xi}^{-2(1+\gamma)}f_{\xi\xi}. \tag{4.3.2}$$

A separation of variables argument implies that:

$$\begin{cases} \frac{\dot{a}}{a}=-\beta\frac{c_0^{-2-2\gamma}}{a^{-2\gamma}}t^{\rho-1} \\ \frac{\dot{b}}{a}=-\lambda\frac{c_0^{-2-2\gamma}}{a^{-2\gamma}}t^{\rho-1} \end{cases}, \tag{4.3.3}$$

where β,λ are arbitrary constants, and $\gamma>\frac{-1}{2}$.

The equation for the profile f (4.3.2) becomes:

$$\left(\beta\xi+\lambda\right)\frac{df}{d\xi}=\left(\frac{df}{d\xi}\right)^{-2(1+\gamma)}\frac{d^2f}{d\xi^2}. \tag{4.3.4}$$

According to different value of parameter γ, we discuss the solutions of (4.3.3) and (4.3.4).

The case: $\gamma>0$:

The resolution of system (4.3.3) is not difficult, indeed from (4.3.3) we have

$$b(t)=\frac{\lambda}{\beta}a(t)+A_1. \tag{4.3.5}$$

If we replace (4.3.5) in (4.3.3), we get

$$\begin{cases} a(t)=\left(\frac{2\gamma\beta}{\rho c_0^{2(1+\gamma)}}t^{\rho}+A_0\right)^{\frac{-1}{2\gamma}} \\ b(t)=\frac{\lambda}{\beta}\left(\frac{2\gamma\beta}{\rho c_0^{2(1+\gamma)}}t^{\rho}+A_0\right)^{\frac{-1}{2\gamma}}+A_1 \end{cases},\ \text{for}\ 0<t<\infty, \tag{4.3.6}$$

for $\beta>0$, and $A_0>0$, A_1 are constants.

The equation for the profile f (4.3.4) can be written as:

$$\left(\frac{df}{d\xi}\right)^{-1-2(1+\gamma)} \frac{d^2 f}{d\xi^2} = (\beta\xi + \lambda), \qquad \text{where } \beta > 0 \text{ and } \lambda \in \mathbb{R},$$

after integration, we obtain

$$\frac{-1}{2(1+\gamma)} \left(\frac{df}{d\xi}\right)^{-2(1+\gamma)} = \beta\frac{\xi^2}{2} + \lambda\xi + k, \quad \text{with } k \text{ constant},$$

and another integration gives

$$\frac{df}{d\xi} = \left[\frac{1}{1+\gamma}\right]^{\frac{1}{2(1+\gamma)}} C^{\frac{-1}{1+\gamma}} \left[1 - \left(\frac{\beta\xi + \lambda}{C\sqrt{\beta}}\right)^2\right]^{\frac{-1}{2(1+\gamma)}}, \tag{4.3.7}$$

for

$$-\frac{\lambda + C\sqrt{\beta}}{\beta} \leq \xi \leq -\frac{\lambda - C\sqrt{\beta}}{\beta}.$$

For $\xi = \frac{x-b(t)}{a(t)}$, this relation suggests a free-boundary problem for determination of the image intensity evolution in the boundary layer $l(t)$ and $r(t)$ such that

$$l(t) = b(t) - \frac{\lambda + C\sqrt{\beta}}{\beta} a(t) \leq x \leq b(t) - \frac{\lambda - C\sqrt{\beta}}{\beta} a(t) = r(t),$$

where $a(t), b(t)$ are given by (4.3.6). If we replace $b(t)$ "given by (4.3.6)" we obtain

$$l(t) = A_1 - \frac{C}{\sqrt{\beta}} a(t) \leq x \leq A_1 + \frac{C}{\sqrt{\beta}} a(t) = r(t).$$

Here, C is an integration constant. Further integration and using the boundary conditions $f\left(-\frac{\lambda+C\sqrt{\beta}}{\beta}\right) = 0$, $f\left(-\frac{\lambda-C\sqrt{\beta}}{\beta}\right) = 1$, then we obtain

$$f(\xi) = \frac{1}{\sqrt{\beta}} \left[\frac{1}{1+\gamma}\right]^{\frac{1}{2(1+\gamma)}} C^{\frac{\gamma}{1+\gamma}} \int_{-1}^{\frac{\beta\xi+\lambda}{C\sqrt{\beta}}} \frac{d\eta}{[1-\eta^2]^{\frac{1}{2(1+\gamma)}}};$$

and

$$C = \left[\frac{2}{\sqrt{\beta}} \left[\frac{1}{1+\gamma}\right]^{\frac{1}{2(1+\gamma)}} \int_0^1 \frac{d\eta}{[1-\eta^2]^{\frac{1}{2(1+\gamma)}}}\right]^{-\frac{\gamma+1}{\gamma}}.$$

Thus, the travelling profiles solutions assumes the form:

$$u\left(x,t\right)=c_0\left[\frac{1}{\sqrt{\beta}}\left[\frac{1}{1+\gamma}\right]^{\frac{1}{2(1+\gamma)}}C^{\frac{\gamma}{1+\gamma}}\int_{-1}^{\sqrt{\beta}\frac{x-A_1}{Ca(t)}}\frac{d\eta}{\left[1-\eta^2\right]^{\frac{1}{2(1+\gamma)}}}\right].$$

The gradients are given by

$$u_x(x,t)=\frac{c_0}{a(t)}f'(\xi),$$

from (4.3.7), we have

$$u_x(x,t)=\frac{c_0}{a(t)}\left[\frac{1}{1+\gamma}\right]^{\frac{1}{2(1+\gamma)}}C^{\frac{-1}{1+\gamma}}\left[1-\left(\sqrt{\beta}\frac{x-A_1}{Ca(t)}\right)^2\right]^{\frac{-1}{2(1+\gamma)}}.$$

$$if\quad t\to\infty,\ then\quad u_x(x,t)\to\infty,\quad (a(t)\to 0).$$

Therefore the validity of the asymptotic equation (4.1) improves with time. Thus, the gradients blow up like $\frac{1}{a(t)}$ or like "$O(t^{\frac{\rho}{2\gamma}})$ " as $t\to\infty$. The width of the transition region $r(t)-l(t)$ equal to $2\frac{C}{\sqrt{\beta}}a(t)=2\frac{C}{\sqrt{\beta}}\left(\frac{2\gamma\beta}{\rho c_0^{2(1+\gamma)}}t^{\rho}+A_0\right)^{\frac{-1}{2\gamma}}$ decreases with time. In this case the phenomenon of gradient enhancement takes place: The spatial gradient of the solutions, u_x, increases with time, and its support shrinks. See figures 20, 21.

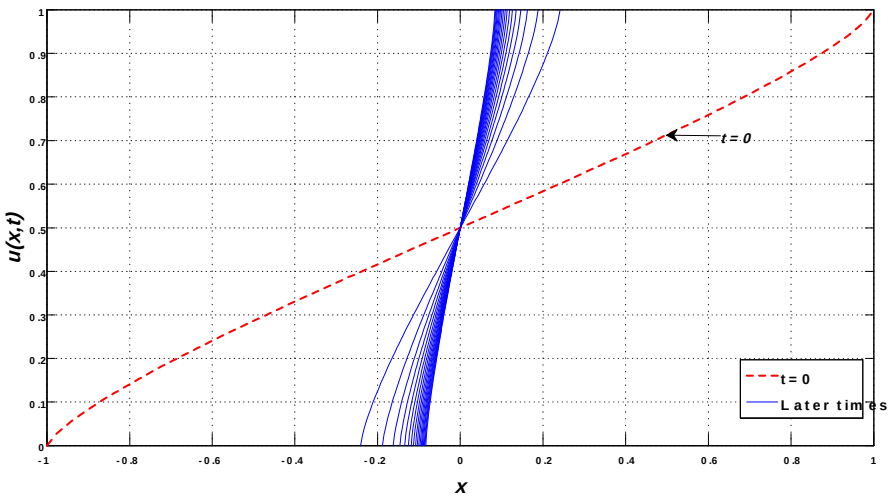

Figure 20: The evolution of the image intensity distribution $u(x,t)$ for $\gamma=1$ and $\rho=\frac{3}{4}$.

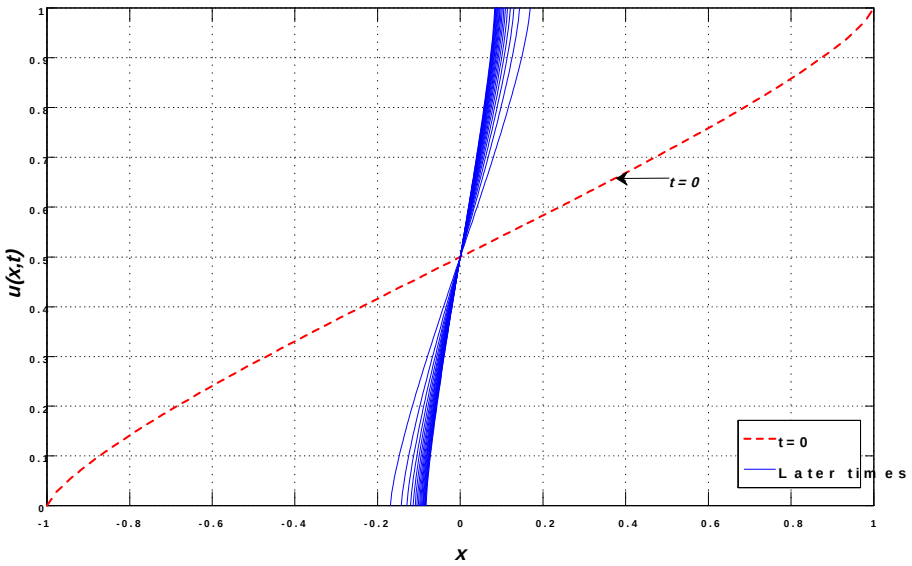

Figure 21: The evolution of the image intensity distribution $u(x,t)$ for $\gamma = 1$ and $\rho = \frac{1}{2}$.

The case: $\gamma = 0$:

The equation (4.1) becomes:

$$D_t^{\rho} u(x,t) = u_x^{-2} u_{xx}. \tag{4.3.8}$$

If we replace the solution (4.3.1) in equation (4.3.8), we obtain

$$-\frac{\dot{a}}{a}\xi f'_{\xi} - \frac{\dot{b}}{a} f'_{\xi} = c_0^{-2} f_{\xi}^{-2} f_{\xi\xi}. \tag{4.3.9}$$

A separation of variables argument implies that the following conditions must hold :

$$\begin{cases} \frac{\dot{a}}{a} = -\beta c_0^{-2} t^{\rho-1} \\ \frac{\dot{b}}{a} = -\lambda c_0^{-2} t^{\rho-1} \end{cases}, \tag{4.3.10}$$

where β, λ are arbitrary constants .

The resolution of system (4.3.10) gives:

$$\begin{cases} a(t) = A_0 e^{-\frac{\beta}{\rho} c_0^{-2} t^{\rho}} \\ b(t) = \frac{\lambda}{\beta} A_0 e^{-\frac{\beta}{\rho} c_0^{-2} t^{\rho}} + A_1 \end{cases}, \text{ for } 0 < t < \infty. \tag{4.3.11}$$

The equation for the profile f becomes:

$$(\beta\xi+\lambda)\frac{df}{d\xi}=\left(\frac{df}{d\xi}\right)^{-2}\frac{d^2f}{d\xi^2}, \tag{4.3.12}$$

which can be written as

$$\left(\frac{df}{d\xi}\right)^{-3}\frac{d^2f}{d\xi^2}=(\beta\xi+\lambda),\qquad \text{where } \beta\in\mathbb{R}_+^*,\lambda\in\mathbb{R},$$

after integration, we obtain

$$\frac{df}{d\xi}=\frac{1}{C}\left[1-\left(\frac{\beta\xi+\lambda}{C\sqrt{\beta}}\right)^2\right]^{\frac{-1}{2}},$$

where $C>0$ is an integration constant. By using the boundary conditions $f\left(-\frac{\lambda+C\sqrt{\beta}}{\beta}\right)=0$, and $f\left(-\frac{\lambda-C\sqrt{\beta}}{\beta}\right)=1$, we obtain, after integration:

$$f(\xi)=\frac{1}{\pi}\arcsin\left(\frac{\pi^2\xi+\lambda}{\pi C}\right)+\frac{1}{2};\quad \beta=\pi^2,$$

for

$$\frac{-C\pi-\lambda}{\pi^2}\leq\xi\leq\frac{C\pi-\lambda}{\pi^2}.$$

Thus, the travelling profiles solutions assumes the form

$$u(x,t)=c_0\left[\frac{1}{\pi}\arcsin\left(\pi\frac{x-A_1}{Ca(t)}\right)+\frac{1}{2}\right];$$

for

$$l(t)=b(t)-\frac{\lambda+C\pi}{\pi^2}a(t)\leq x\leq b(t)-\frac{\lambda-C\pi}{\pi^2}a(t)=r(t),$$

where $a(t)$ and $b(t)$ are given by (4.3.11). We can write:

$$l(t)=A_1-\frac{C}{\pi}a(t)\leq x\leq A_1+\frac{C}{\pi}a(t)=r(t).$$

The gradients are given by

$$u_x(x,t)=\frac{c_0}{a(t)}f'(\xi)=\frac{c_0}{Ca(t)}\left[1-\left(\pi\frac{x-A_1}{Ca(t)}\right)^2\right]^{\frac{-1}{2}}.$$

$$\text{if} \quad t \to \infty, \ \text{we have} \ \ u_x(x,t) \to \infty, \ \ (for \ a(t) \to 0).$$

Thus; The gradients blow up exponentially as $t \to \infty$. The width of the transition region $r(t) - l(t)$ is given by $2\frac{C}{\pi}A_0 e^{-\left(\frac{\pi}{\sqrt{\rho}c_0}\right)^2 t^\rho}$ decreases with time. In this case the phenomenon of edge enhancement takes place for this class of equations ($\gamma = 0$), see figures 22, 23.

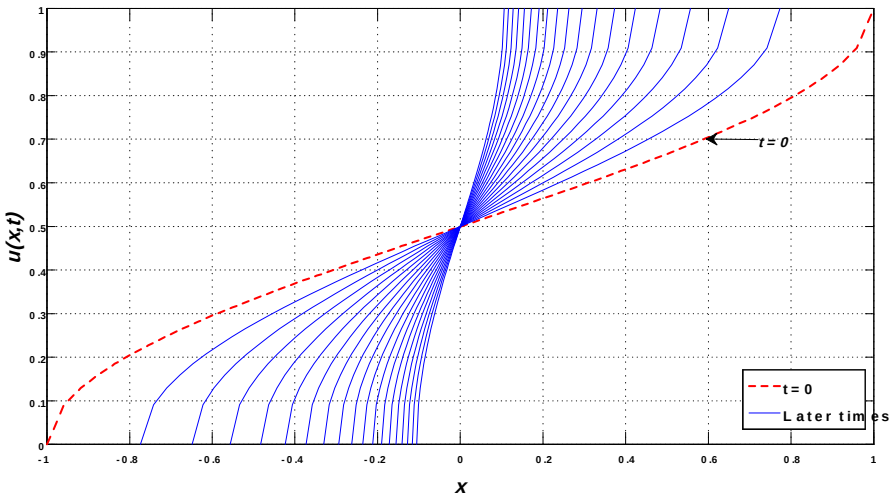

Figure 22: The evolution of the image intensity distribution $u(x,t)$ for $\gamma = 0$ and $\rho = \frac{3}{4}$.

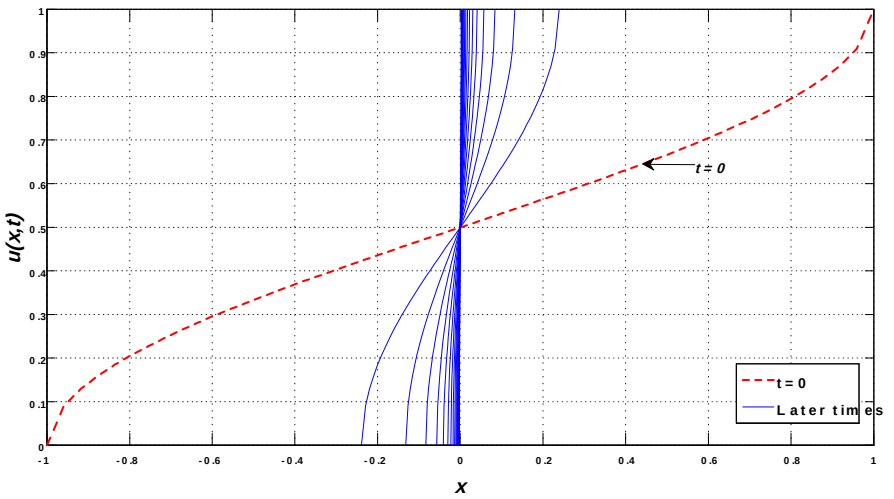

Figure 23: The evolution of the image intensity distribution $u(x,t)$ for $\gamma = 0$ and $\rho = \frac{1}{2}$.

The case: $\frac{-1}{2} < \gamma < 0$:

In this case, the parameters $a(t)$ and $b(t)$ are given from (4.3.3) by :

$$\begin{cases} a(t) = \left(\frac{2\gamma\beta}{\rho c_0^{2(1+\gamma)}} t^\rho + A_0\right)^{\frac{-1}{2\gamma}} \\ b(t) = \frac{\lambda}{\beta}\left(\frac{2\gamma\beta}{\rho c_0^{2(1+\gamma)}} t^\rho + A_0\right)^{\frac{-1}{2\gamma}} + A_1 \end{cases}, \quad 0 < t < T = \left[-\frac{\rho A_0 c_0^{2(1+\gamma)}}{2\gamma\beta}\right]^{\frac{1}{\rho}}, \qquad (4.3.13)$$

with $\frac{-1}{2} < \gamma < 0$, and $\beta > 0$, where $A_0 > 0$, A_1 are a constants.

The solution of equation for the profile f (4.3.4), is given by:

$$f(\xi) = \frac{1}{\sqrt{\beta}}\left[\frac{1}{1+\gamma}\right]^{\frac{1}{2(1+\gamma)}} C^{\frac{\gamma}{1+\gamma}} \int_{-1}^{\frac{\beta\xi+\lambda}{C\sqrt{\beta}}} \frac{d\eta}{[1-\eta^2]^{\frac{1}{2(1+\gamma)}}}; \quad \text{for } \frac{-1}{2} < \gamma < 0,$$

with

$$\frac{-C\sqrt{\beta}-\lambda}{\beta} \le \xi \le \frac{C\sqrt{\beta}-\lambda}{\beta}.$$

The relation for C is given also by:

$$C = \left[\frac{2}{\sqrt{\beta}}\left[\frac{1}{1+\gamma}\right]^{\frac{1}{2(1+\gamma)}} \int_0^1 \frac{d\eta}{[1-\eta^2]^{\frac{1}{2(1+\gamma)}}}\right]^{-\frac{\gamma+1}{\gamma}}, \ \frac{-1}{2} < \gamma < 0.$$

Returning to the variables x and t we obtain the travelling profiles solutions as follow:

$$u(x,t) = c_0\left[\frac{1}{\sqrt{\beta}}\left[\frac{1}{1+\gamma}\right]^{\frac{1}{2(1+\gamma)}} C^{\frac{\gamma}{1+\gamma}} \int_{-1}^{\sqrt{\beta}\frac{x-A_1}{Ca(t)}} \frac{d\eta}{[1-\eta^2]^{\frac{1}{2(1+\gamma)}}}\right], \ \frac{-1}{2} < \gamma < 0,$$

for free boundaries:

$$l(t) = b(t) - \frac{\lambda + C\sqrt{\beta}}{\beta} a(t) \le x \le b(t) - \frac{\lambda - C\sqrt{\beta}}{\beta} a(t) = r(t),$$

where $a(t), b(t)$ are given by (4.3.13). We can simply write:

$$l(t) = A_1 - \frac{C}{\sqrt{\beta}} a(t) \le x \le A_1 + \frac{C}{\sqrt{\beta}} a(t) = r(t).$$

The gradients are given by

$$u_x(x,t) = \frac{c_0}{a(t)} f'(\xi) = \frac{c_0}{a(t)} \left[\frac{1}{1+\gamma}\right]^{\frac{1}{2(1+\gamma)}} C^{\frac{-1}{1+\gamma}} \left[1 - \left(\sqrt{\beta}\frac{x - A_1}{Ca(t)}\right)^2\right]^{\frac{-1}{2(1+\gamma)}}.$$

In this case $lim\ a(t) = 0$, if $t \to T$, then we have:

$$u_x(x,t) \to \infty, \text{ for } t \to T.$$

Therefore the validity of the asymptotic equation (4.1) improves with time: The gradients blow up like $\left(\frac{2\gamma\beta}{\rho c_0^{2(1+\gamma)}} t^\rho + A_0\right)^{\frac{1}{2\gamma}}$ or like "$O((T-t)^{\frac{\rho}{2\gamma}})$ " as $t \to T$ The width of the transition region $r(t) - l(t)$ is given by $2\frac{C}{\sqrt{\beta}} \left(\frac{2\gamma\beta}{\rho c_0^{2(1+\gamma)}} t^\rho + A_0\right)^{\frac{-1}{2\gamma}}$ decreases with time for $0 < t < T$. See figures 24, 25.

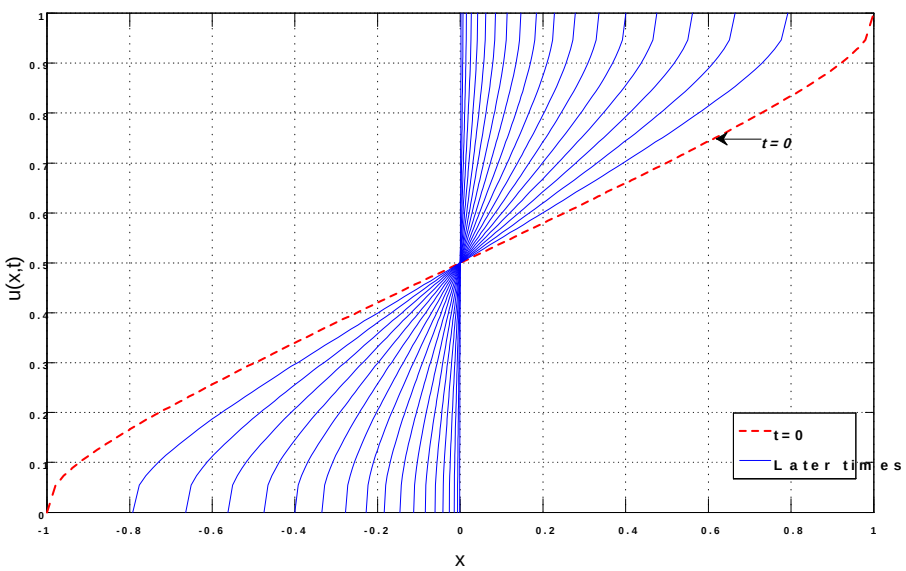

Figure 24: The evolution of the image intensity distribution $u(x,t)$ for $\gamma = \frac{-1}{4}$ and $\rho = \frac{3}{4}$.

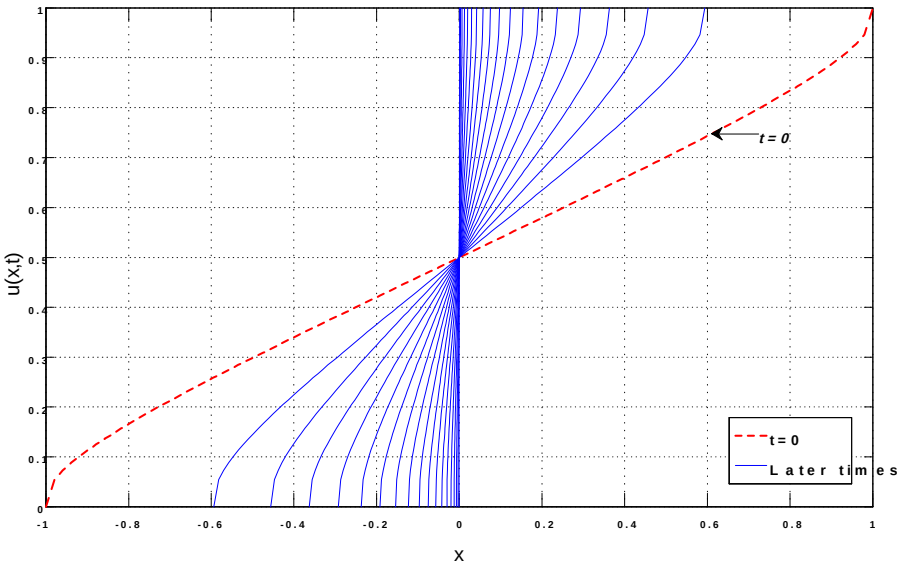

Figure 25: The evolution of the image intensity distribution $u(x,t)$ for $\gamma = \frac{-1}{4}$ and $\rho = \frac{1}{2}$.

Case2: $\alpha = \beta \in \mathbb{R},\ \lambda \in \mathbb{R}$:

Now we discuss another case, so we assume that

$$\int_{\mathbb{R}} u(s,t)\, ds = const,$$

We can see that from (3.0.1), we have

$$\int_{\mathbb{R}} u(s,t)\, ds \ = \int_{\mathbb{R}} c(t)\, f\left(\frac{s-b(t)}{a(t)}\right) ds = a(t)\, c(t) \int_{\mathbb{R}} f(\xi)\, d\xi = const,$$

this implies

$$c(t) = \frac{const}{a(t)}, \tag{4.3.14}$$

from relation (4.2.4) and (4.3.14), we have then $\alpha = \beta$, this case corresponds to physical law (conservation of mass).

In this case, new explicit solutions are obtained to equation (4.1), which depends of parameter γ.

The case: $\gamma \in \left]\frac{-1}{2}; \infty\right[- \{0\}$:

The equation of profile f (4.2.3) becomes:

$$f_\xi^{-2(1+\gamma)} f_{\xi\xi} = \left[(\beta\xi + \lambda)\, f\right]_\xi, \qquad \text{where } \alpha, \lambda \in \mathbb{R}. \tag{4.3.15}$$

After integration, we obtain:

$$\frac{-1}{2\gamma+1} f_\xi^{-2\gamma-1} = (\beta\xi + \lambda)\, f + k, \text{ with } k \text{ is constant.}$$

If we put for example $f(0) = f_\xi(0) = 0$, this implies $k = 0$, we obtain:

$$f_\xi^{-2\gamma-1} = -(2\gamma+1)(\beta\xi + \lambda)\, f,$$

this implies,

$$f^{\frac{1}{2\gamma+1}} df = \left((2\gamma+1)(-\beta\xi - \lambda)\right)^{\frac{-1}{2\gamma+1}} d\xi.$$

Integrating once more, we get

$$\frac{2\gamma+1}{2\gamma+2} f^{\frac{2\gamma+2}{2\gamma+1}} = \frac{(2\gamma+1)^{\frac{2\gamma}{2\gamma+1}}}{-2\gamma\beta} (-\beta\xi - \lambda)^{\frac{2\gamma}{2\gamma+1}} + K,$$

where K is an integration constant.

Then, the solution of (4.3.15) is written under the form:

$$\begin{aligned} f(\xi) = &\left[(2\gamma+2)(2\gamma+1)^{\frac{1}{2\gamma+1}}\right]^{\frac{2\gamma+1}{2\gamma+2}} \times \\ &\left[\left(\tfrac{-1}{2\gamma\beta}\left[(-\beta\xi - \lambda)_+\right]^{\frac{2\gamma}{2\gamma+1}} + K\right)_+\right]^{\frac{2\gamma+1}{2\gamma+2}}, \quad \text{for } \gamma \in \left]\tfrac{-1}{2}; \infty\right[- \{0\}. \end{aligned}$$

Finally, an explicit exact solution to the nonlinear degenerate parabolic equation (4.1) is given as follows:

$$\begin{aligned} u(x,t) = c(t) &\left[(2\gamma+1)^{\frac{2\gamma+2}{2\gamma+1}}\right]^{\frac{2\gamma+1}{2\gamma+2}} \times \\ &\left[\left(\tfrac{-1}{2\gamma\beta}\left[(-\beta\tfrac{x-b(t)}{a(t)} - \lambda)_+\right]^{\frac{2\gamma}{2\gamma+1}} + K\right)_+\right]^{\frac{2\gamma+1}{2\gamma+2}}. \end{aligned} \tag{4.3.16}$$

The coefficients $c(t), a(t)$ and $b(t)$ are given, explicitly, by:

$$\begin{cases} a(t) = \left[K_0^{-2-2\gamma}\frac{S\beta}{\rho} t^\rho + A_0\right]^{\frac{-1}{S}} \\ c(t) = K_0\left[K_0^{-2-2\gamma}\frac{S\beta}{\rho} t^\rho + A_0\right]^{\frac{1}{S}} \\ b(t) = \frac{\lambda}{\alpha}\left[K_0^{-2-2\gamma}\frac{S\beta}{\rho} t^\rho + A_0\right]^{\frac{-1}{S}} + A_1 \end{cases}, \quad \textit{for } 0 < t < T, \textit{ and } \alpha = \beta < 0, \tag{4.3.17}$$

with

$$T=\left[-\frac{\rho A_0 K_0^{2+2\gamma}}{S\beta}\right]^{\frac{1}{\rho}}.$$

And

$$\begin{cases} a(t)=\left[K_0^{-2-2\gamma}\frac{S\beta}{\rho}t^{\rho}+A_0\right]^{\frac{-1}{S}} \\ c(t)=K_0\left[K_0^{-2-2\gamma}\frac{S\beta}{\rho}t^{\rho}+A_0\right]^{\frac{1}{S}} \\ b(t)=\frac{\lambda}{\alpha}\left[K_0^{-2-2\gamma}\frac{S\beta}{\rho}t^{\rho}+A_0\right]^{\frac{-1}{S}}+A_1 \end{cases}, \quad \textit{for } 0<t<\infty, \textit{ and } \alpha=\beta>0, \tag{4.3.18}$$

where $S=2(1+2\gamma)>0$, for $\gamma\in\left]\frac{-1}{2};\infty\right[-\{0\}$ and $A_0,K_0>0$, A_1 are constants.

The case: $\gamma=0$:

Clearly, if we set $\gamma=0$, in (4.2.5) and (4.2.6), the coefficients $c(t), a(t)$ and $b(t)$ are given by:

$$\begin{cases} a(t)=\left[K_0^{-2}\frac{2\alpha}{\rho}t^{\rho}+A_0\right]^{\frac{-1}{2}} \\ c(t)=K_0\left[K_0^{-2}\frac{2\alpha}{\rho}t^{\rho}+A_0\right]^{\frac{1}{2}} \\ b(t)=\frac{\lambda}{\alpha}\left[K_0^{-2}\frac{2\alpha}{\rho}t^{\rho}+A_0\right]^{\frac{-1}{2}}+A_1 \end{cases}, \quad \textit{for } 0<t<T, \textit{ and } \beta=\alpha<0, \tag{4.3.19}$$

with

$$T=\left[-\frac{\rho A_0 K_0^{2}}{2\alpha}\right]^{\frac{1}{\rho}}.$$

And

$$\begin{cases} a(t)=\left[K_0^{-2}\frac{2\alpha}{\rho}t^{\rho}+A_0\right]^{\frac{-1}{2}} \\ c(t)=K_0\left[K_0^{-2}\frac{2\alpha}{\rho}t^{\rho}+A_0\right]^{\frac{1}{2}} \\ b(t)=\frac{\lambda}{\alpha}\left[K_0^{-2}\frac{2\alpha}{\rho}t^{\rho}+A_0\right]^{\frac{-1}{2}}+A_1 \end{cases}, \quad \textit{for } 0<t<\infty, \textit{ and } \beta=\alpha>0, \tag{4.3.20}$$

where $A_0,K_0>0$, A_1 are constants.

The equation of profile f (4.2.3) becomes:

$$f_{\xi}^{-2}f_{\xi\xi}=\left[(\alpha\xi+\lambda)f\right]_{\xi}, \qquad \text{where } \alpha,\lambda\in\mathbb{R}. \tag{4.3.21}$$

Integration of (4.3.21) and putting $f(0) = f_\xi(0) = 0$; after a routine computation this yields

$$f_\xi f = \frac{-1}{\alpha\xi + \lambda}.$$

Integrating once more, we obtain:

$$\frac{1}{2}f^2 = \frac{-1}{\alpha}\ln|\alpha\xi + \lambda| + K,$$

where K is an integration constant.

Therefore, the solution of (4.3.21) is written under the form:

$$f(\xi) = \left[\left(\frac{-2}{\alpha}\ln|\alpha\xi + \lambda| + K\right)_+\right]^{\frac{1}{2}},$$

Returning to the variables x and t we obtain:

$$u(x,t) = c(t)\left[\left(\frac{-2}{\alpha}\ln\left|\alpha\frac{x - b(t)}{a(t)} + \lambda\right| + K\right)_+\right]^{\frac{1}{2}}.$$

where $c(t), a(t)$ and $b(t)$ are given by (4.3.19) and (4.3.20).

4.4 Comments and Conclusion

In this chapter we have presented some explicit exact solutions to a nonlinear fractional diffusion and its application in contour enhancement in image processing. We have introduced a general form of self similar solutions, called "travelling profiles solutions". We have also given a generalize results obtained for a free boundary problem investigated in previous chapters, to study the contour enhancement in image processing. We have obtained new results in the larger range of fractional derivative $\rho \in (0, 1]$. We note that, the particular cases studied in chapter 2 and 3, it coincides if we set $\rho = 1$.

Conclusion

In this thesis, we are interested in a free boundary problem appearing in contour image enhancing via partial differential equation. The technique used in this work is seeking general self-similar solutions, to describe the phenomenon of contour enhancement in image processing. The originality of this work consists in generalizing the results obtained by Barenblatt and Vasquez [4, 3], these authors have constructed a free boundary problem for the model proposed by Mallladi and Sethian [21] simplified and reduced in one dimension, seeking solutions to this problem in form "intermediate-asymptotic self-similar solution", they arrived to demonstrate the enhancement of contour via the evolution of the support of the image intensity function, and that for positive values of the parameter of enhancement of contour.

In this work, we have generalized the results obtained in [4, 3], by introducing general self-similar solutions, and we have used a simple and direct method, demonstrate above all that the contour enhancement phenomenon can also occur for negative values. Another most interesting generalization concerns the introduction of so-called Travelling profiles solutions. We have obtained new exact solutions for the equation describe the evolution on the function of image intensity, whose contour enhancement results were obtained for a negative values of parameter. These new forms of solution offer us new perspectives in the study of this type of problem if one succeeds in clarifying the role of the parameter and the amplitude in the study of contour of image.

Finally, we have proposed another generalization, based on the mathematical model itself, introducing fractional derivatives in the basic equation, a detailed study is presented in this thesis and interesting results have been obtained.

The results obtained in this work, (one-dimensional case), can be confirmed in 2-D by using numerical methods, that is our objective in the future studies.

Bibliography

[1] Alvarez, L., Lions, P.L. and Morel, J.M. (1992) '*Image selective smoothing and edge detection by nonlinear diffusion. II*', Society for Industrial and Applied Mathematics. Journal on Numerical Analysis, Vol.29, No.3, pp.845–866.

[2] Aubert, G., Kornprobst, P. (2006) '*Mathematical Problems in. Image Processing. Partial Differential Equations and the. Calculus of Variations*', Springer-Verlag New York, Inc. Secaucus, NJ, USA.

[3] Barenblatt, G.I. (2001) '*Self-similar intermediate asymptotics for nonlinear degenerate parabolic free-boundary problems that occur in image processing*', Proceedings of the National Academy of Sciences of the United States of America, Vol.98, No.23, pp.12878–12881.

[4] Barenblatt, G.I. and Vazquez, J. L. (2003) '*Nonlinear diffusion and image contour enhancement*', Interfaces and Free Boundaries, Vol.6, No.1, pp.31-54.

[5] Benhamidouche, N. (2008) '*Exact solutions to some nonlinear PDEs, travelling profiles method*', Electronic Journal of Qualitative Theory of Differential Equation, No.15, pp.1-7.

[6] Benhamidouche, N. and Arioua, Y. (2009) '*New Method for Constructing Exact Solutions to Nonlinear PDEs*', International Journal of Nonlinear Science, Vol.7, No.4, pp.395-398.

[7] Black, M.J., Sapiro G., Marimont D.H., and Heeger, D. (1998) '*Robust anisotropic diffusion*', IEEE Trans, on Image Process, Vol.7, pp.421-432.

[8] Canny, J. (1986) '*A computational approach to edge detection*', IEEE Trans, on Pattern Anal. Machine Intelligence, Vol.8, pp.679-698.

[9] Catté, F., Lions, P.-L., Morel, J.M. and Coll, T. (1992) '*Image Selective Smoothing and Edge Detection by Nonlinear Diffusion*', SIAM J. Numer. Anal., Vol.29 , pp.182-193.

[10] Charbonnier, P., Blanc-Feraud, L., Aubert, G. and Barlaud, M. (1994) '*Two deterministic half-quadratic regularization algorithms for computed imaging*', Proc. IEEE Int. Conf. Image Processing (ICIP-94, Austin, Nov.13-16, 1994) IEEE Computer Society Press, Los Alamitos, Vol.2, pp.168-172.

[11] Chouder, R. and Benhamidouche, N. (in press) '*New exact solutions to nonlinear diffusion equation that occurs in image processing*', International Journal of Computing Science and Mathematics.

[12] Diethelm, K. (2010) '*The Analysis of Fractional Differential Equations An Application Oriented Exposition Using Differential Operators of Caputo Type*', Springer-Verlag Berlin Heidelberg.

[13] Fischl, B. and Schwartz, E.L. (1997) '*Learning an integral equation approximation to nonlinear anisotropic diffusion in image processing*'. IEEE Trans, on Pattern Anal. Machine Intelligence Vol.19, pp.342-352.

[14] Herzallah, M.A.E., El-Sayed, A.M.A. and Baleanu, D. (2010) '*On the fractional-order Diffusion-Wave process*', Romanian Journal of Physics, Vol.55, No.(3–4), pp.274-284.

[15] Hilfer, R. (2000) '*Applications of Fractional Calculus in Physics*', World Scientific, New Jersey.

[16] Katugampola, U.N. (2011) '*New approach to a generalized fractional integral*', Appl. Math. Comput., Vol.218, No.3, pp.860–865.

[17] Khalil, R., Horani, M.A., Yousef, A. and Sababheh, M. (2014) '*A new definition of fractional derivative*', J. Comput. Appl. Math. Vol.264, pp.65–70.

[18] Kilbas, A.A., Srivastava, H.M. and Trujillo, J.J. (2006) '*Theory and Applications of Fractional Differential Equations*', North-Holland Mathematical Studies, Elsevier, Amsterdam.

[19] Koenderink, J. (1984) '*The structure of images*', Biol. Cybern Vol.50, pp.363-370.

[20] Leibniz, G.W. (1962) '*Letter from Hanover, Germany to G.F.A. L'Hospital, September 30, 1695*', Leibniz Mathematische Schriften, Olms-Verlag, Hildesheim, Germany, p.301-302, First published in 1849.

[21] Malladi, R. and Sethian, J.A. (1996) '*Image Processing: Flows under Min/Max curvature and Mean Curvature*', Graphical Models and Image Processing, Vol.58, No.2, pp.127–141.

[22] Miller, K.S. and Ross, B. (1993) '*An Introduction to the Fractional Calculus and Fractional Differential Equations*', John Wiley & Sons, New York.

[23] Nordstrom, K.N. (1990) '*Biased anisotropic diffusion: a unified regularization and diffusion approach to edge detection*'. Image and Vision Computing, Vol.8, pp.318-327.

[24] Oldham, K.B. and Spanier, J. (1974) '*The fractional calculus*', Academic Press, New York.

[25] Perona, P. and Malik, J. (1987) '*Scale-space and edge detection using anisotropic diffusion*', IEEE Transactions on Pattern Analysis and Machine Intelligence, Vol.12, No.7, pp.629–639.

[26] Podlubny, I. (1999) '*Fractional Differential Equations*', Acad. Press, San Diego - New York - London.

[27] Samko, S.G., Kilbas, A.A. and Marichev, O.I. (1993) '*Fractional Integrals and Derivatives: Theory and Applcations*', Gordon and Breach, New York, Translated from the Russian edition, Minsk (1987).

[28] Sochen, N., Kimmel, R. and Malladi, R. (1996) '*From high energy physics to low level vision*'. Preprint LBNL-39243, UC-405, E. O. Lawrence Berkeley National Laboratory, pp.38.

[29] Tarasov, V.E. (2010) '*Fractional Dynamics Applications of Fractional Calculus to Dynamics of Particles, Fields and Media*', Higher Education Press, Beijing and Springer-Verlag Berlin Heidelberg.

[30] Weickert, J. (1998) '*Anisotropic Diffusion in Image Processing*'. Stuttgart: BG: Teubner Stuttgart.

[31] Witkin, A.P. (1983) '*Scale-space filtering*', Presented at 8th int. Joint conf. Art. intell., Karlsruhe, Germany.

[32] You, Y., Xu, W., Tannenbaum, A. and Kaveh, M. (1996) '*Behavioral analysis of anisotropic diffusion in image processing*'. IEEE Trans, on Image Process Vol.5, pp.1539-1552.

Abstract

The theory of nonlinear diffusion equations is used to analyze the process of contour enhancement in image processing. The aim of this research is to seek new exact solutions to nonlinear diffusion equation that occurs in image processing called degenerate parabolic equation. For that, we have used the general self-similar solutions and the `travelling profiles method' in order to find, explicitly, new exact solutions to this equation under some conditions. Some these explicit solutions are related with the phenomenon of contour enhancement. An interesting particular case has been discussed; this case coincides with particular solutions called `intermediate asymptotic solutions' used to study the contour enhancement.

Keywords: nonlinear diffusion equations; self similar solution; travelling profiles method; fractional derivatives; image processing; contour enhancement.

Résume

La théorie des équations de diffusion non linéaires est utilisée pour analyser le processus d'amélioration de contour en traitement de l'image. Le but de la présente recherche est de chercher de nouvelles solutions exactes d'équation de diffusion non linéaire qui apparaître dans le traitement de l'image appelée équation parabolique dégénérée. Pour ça, nous avons utilisé les solutions auto-similaires générales et la méthode de profiles mobiles pour trouver, explicitement, de nouvelles solutions exactes de cette équation sous quelques conditions. Ces solutions explicites sont liées avec les phénomènes d'amélioration de contour. Un cas particulier intéressant a été discuté; ce cas coïncide avec les solutions particulières appelées 'solutions asymptotiques intermédiaires' utilisées pour étudier l'amélioration de contour.

Mots-clés: Les équations de diffusion non linéaires ; solutions auto-similaires ; la méthode de profiles mobiles ; dérivées fractionnaires ; traitement de l'image ; amélioration de contour.

الملخص

نظرية معادلات الانتشار غير الخطية تستعمل في تحليل عملية تحسين الحواف في معالجة الصورة. الهدف من هذه الأطروحة هو البحث عن حلول دقيقة جديدة لمعادلة الانتشار غير الخطية التي تظهر في معالجة الصور والتي تسمى معادلة قطعية مكافئة منحطة. لهذا استعملنا الحلول المماثلة ذاتيا العامة و طريقة الأشكال المتنقلة لإيجاد، ببساطة، حلول دقيقة جديدة لهذه المعادلة مع بعض الشروط. هذه الحلول مرتبطة بظاهرة تحسين الحواف. حالة خاصة مهمة نوقشت، هذه الحالة تتصادف مع الحلول الخاصة المسماة ' الحلول التقاربية المتوسطة' المستعملة لدراسة تحسين الحواف.

الكلمات المفتاحية: معادلات الانتشار غير الخطية، الحلول المماثلة ذاتيا، طريقة الأشكال المتنقلة، المشتقات الكسرية، معالجة الصور، تحسين الحواف.